

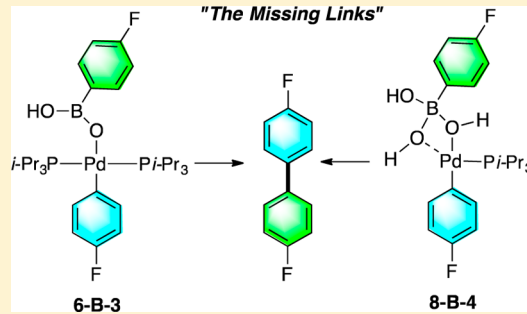
Structural, Kinetic, and Computational Characterization of the Elusive Arylpalladium(II)boronate Complexes in the Suzuki–Miyaura Reaction

Andy A. Thomas,¹⁰ Hao Wang, Andrew F. Zahrt, and Scott E. Denmark^{*10}

Roger Adams Laboratory, Department of Chemistry, University of Illinois, Urbana, Illinois 61801, United States

Supporting Information

ABSTRACT: The existence of the oft-invoked intermediates containing the crucial Pd–O–B subunit, the “missing link”, has been established in the Suzuki–Miyaura cross-coupling reaction. The use of low-temperature, rapid injection NMR spectroscopy (RI-NMR), kinetic studies, and computational analysis has enabled the generation, observation, and characterization of these highly elusive species. The ability to confirm the intermediacy of Pd–O–B-containing species provided the opportunity to clarify mechanistic aspects of the transfer of the organic moiety from boron to palladium in the key transmetalation step. Specifically, these studies establish the identity of two different intermediates containing Pd–O–B linkages, a tri-coordinate (6-B-3) boronic acid complex and a tetra-coordinate (8-B-4) boronate complex, both of which undergo transmetalation leading to the cross-coupling product. Two distinct mechanistic pathways have been elucidated for stoichiometric reactions of these complexes: (1) transmetalation via an unactivated 6-B-3 intermediate that dominates in the presence of an excess of ligand, and (2) transmetalation via an activated 8-B-4 intermediate that takes place with a deficiency of ligand.



1. INTRODUCTION

Palladium-catalyzed cross-coupling reactions such as the Kumada–Tamao–Corriu¹ (Mg), Suzuki–Miyaura² (B), Stille–Migita–Kosugi³ (Sn), Hiyama–Denmark⁴ (Si), and Negishi⁵ (Zn) reactions have fundamentally changed the practice of organic synthesis in both academic and industrial settings alike (Figure 1).⁶ Among these reactions, the Nobel Prize-sharing Suzuki–Miyaura reaction is the premier cross-coupling process, utilized across all disciplines of chemistry as well as in the industrial synthesis of fine chemicals⁷ and pharmaceuticals⁸ owing to its demonstrated reliability, broad functional group compatibility, and access to a wide variety of commercially available boron-based reagents. At a fundamental level, all of these reactions share the same basic catalytic cycle, comprised of three elementary steps: oxidative addition, transmetalation, and reductive elimination. The oxidative addition and reductive elimination steps are common to all cross-coupling variants; however, because the organometallic donor is involved only in the transmetalation step, it is this event that preparatively and mechanistically differentiates all of these processes.

The desire to understand the relationship between chemical structure and reactivity has led to many mechanistic investigations of these elementary steps. Particularly, the oxidative addition⁹ and reductive elimination¹⁰ steps have been extensively studied, and those insights are applicable to all of the cross-coupling reactions. However, except for the Stille¹¹ and more recently the Hiyama–Denmark¹² couplings, far less is

known about the intricate details of the transmetalation step for these cross-coupling reactions.

The formation of transient, pre-transmetalation intermediates (Pd–O–M linkages) on the borderline of existence makes their observation and especially isolation difficult in practice. As

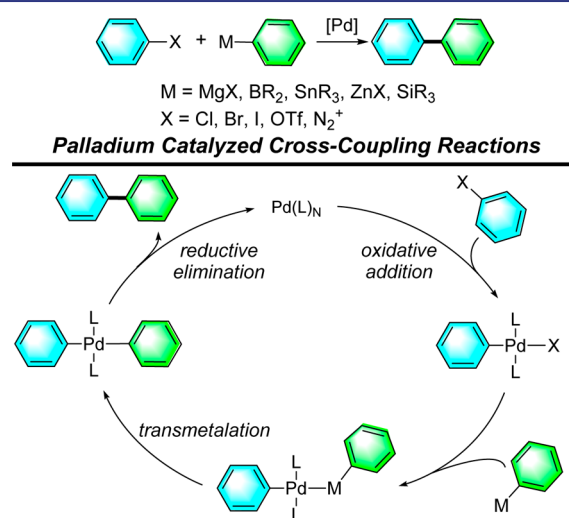


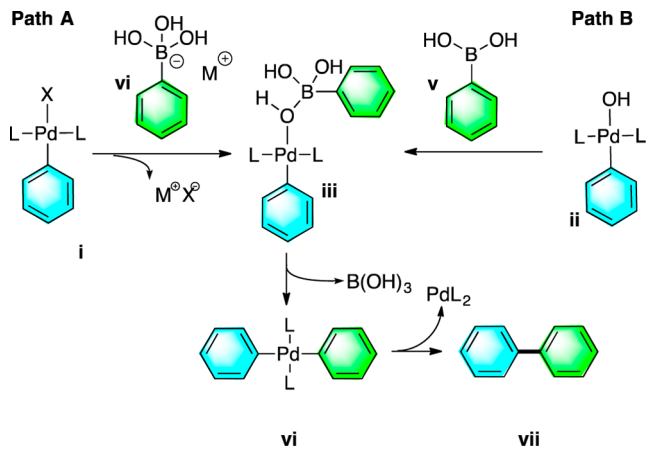
Figure 1. Palladium-catalyzed cross-coupling reactions and general mechanism.

Received: December 30, 2016

a result, reaction kinetics, supported by computational modeling, are often used to investigate the mechanism. Because assumptions must be made about the identity of such intermediates with these experimental methods, the characterization or isolation of a putative intermediate would provide compelling evidence for their existence. However, here again, model compounds must be kinetically validated to demonstrate that the intermediate species is truly on the proposed reaction pathway.

Despite the ubiquitous practice of the Suzuki–Miyaura reaction, a fundamental understanding of the transfer of the organic fragment from boron to palladium remains elusive. Since the discovery of this reaction, two mechanistic pathways (Path A and Path B, Scheme 1) that differ in the role of hydroxide ion have been proposed to initiate the transmetalation event. If the “missing link” (intermediates such as **iii**) between the starting materials and products could be identified, it would provide an unprecedented opportunity to directly interrogate the transmetalation step. Specifically, it would provide insights into the structural features that influence the rate of transmetalation from boron to palladium, which is often the turnover-limiting step.¹³

Scheme 1



Building upon our recent mechanistic investigations on the transmetalation step in palladium-catalyzed coupling of organosilanolate salts,¹² a program of study was undertaken to structurally, kinetically, and computationally characterize arylpalladium(II) arylboronate complexes in the Suzuki–Miyaura reaction. If these intermediates could be prepared and characterized, then their kinetic competence could be established with various ligand systems, and the comparison of these rates of transmetalation could be used to improve reaction design, especially phosphine ligand selection, along with other critical parameters for this cross-coupling process.

2. BACKGROUND

2.1. Pathways for Transmetalation. Currently, two alternative processes (Path A and Path B) have been proposed to initiate the transmetalation event which differ in the precise role of the hydroxide ion which is required for the reaction to proceed.^{14,15} Path A, the “boronate pathway”, proceeds through saturation of the boron valence in **1** to yield a metal trihydroxyarylboronate salt **2**, which then displaces halide from the oxidative addition product **3**, generating species **4** containing the critical Pd–O–B linkage. Path B, the “oxo-

palladium pathway”, proceeds through displacement of halide from the oxidative addition product **3** by hydroxide, thus creating a palladium hydroxide complex **5**, which then combines with the Lewis acidic arylboronic acid **1**, forging the same pre-transmetalation intermediate **4** (Figure 2).

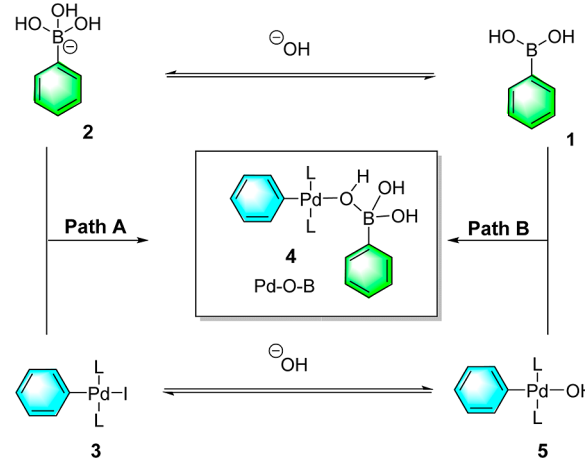
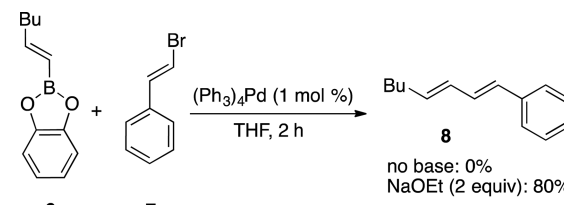


Figure 2. Proposed transmetalation pathways in the Suzuki–Miyaura coupling process.

2.1.1. Early Experimental Evidence for the Transmetalation Event. In 1979, Suzuki and Miyaura examined the formation of 1,3-dienes by cross-coupling reactions between alkenylboranes and bromoalkenes in the presence of $(\text{Ph}_3\text{P})_4\text{Pd}$ as the catalyst.¹⁶ They observed that alkenylboronate **6** and (*E*)- β -bromostyrene **7** failed to react in the absence of alkoxide bases, presumably because of the poor transmetalation reactivity of a non-nucleophilic, tri-coordinate alkenylboronate. However, upon the addition of NaOEt (2.0 equiv), the cross-coupling process was activated, and product **8** was obtained in an 80% yield (Scheme 2). Initially the base was proposed to react with the Lewis acidic boron center to give a more nucleophilic boronate (Path A),¹⁷ which is then capable of transferring its organic group to palladium.

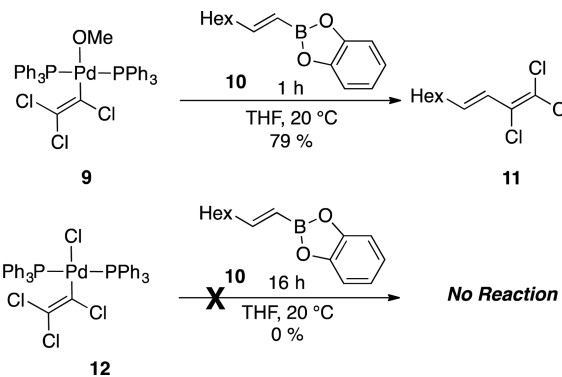
Scheme 2



In 1985, Suzuki and Miyaura established that preformed alkoxy-palladium complex **9** reacted with alkenylboronate **10** to form **11**, whereas chloropalladium complex **12** did not (Scheme 3).¹⁸ The suggestion that the base was capable of activating the palladium center prior to transmetalation (Path B) created a controversy that is still not fully settled. In any event, these studies did not provide unambiguous evidence for the intermediacy of species containing a discrete Pd–O–B linkage.

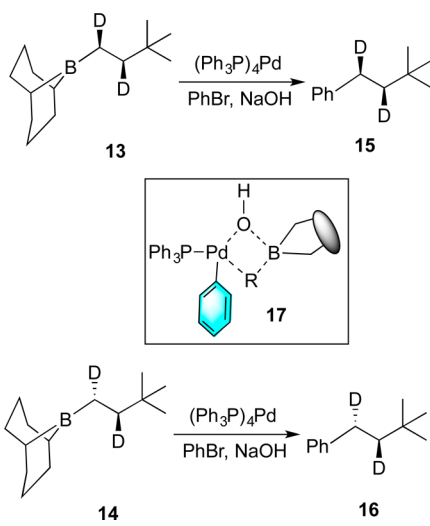
Preliminary evidence for the involvement of a Pd–O–B moiety was provided by an early investigation by Soderquist¹⁹ in which the diastereospecificity of the transmetalation step was examined. Subjecting both *syn* (**13**) and *anti* (**14**) deuterium-

Scheme 3



labeled isomers of *B*-(3,3-dimethyl-1,2-dideutero-1-butyl)-9-BBN to standard Suzuki–Miyaura cross-coupling conditions (THF, NaOH, $(\text{Ph}_3\text{P})_4\text{Pd}$) led to complete retention of configuration in the coupling product (**Scheme 4**). Although no pre-transmetalation intermediate was observed, the retention of configuration indirectly establishes that a Pd–O–B linkage is involved in the transmetalation event.

Scheme 4



2.1.2. Computational Studies. Distinguishing the way in which Pd–O–B linkages are formed in the Suzuki–Miyaura reaction has proven to be challenging, as mechanistic studies are complicated by biphasic reaction conditions (e.g., THF and aqueous base) and by the poor solubility of inorganic bases and metal organoboronate salts in many organic solvents. Consequently, density functional theory (DFT) computational studies have provided insights that suggest Path A is responsible for the formation of pre-transmetalation intermediates. Interestingly, in Ph_3P -ligated complexes, Maseras and Ujaque²⁰ have calculated that the displacement of bromide from the oxidative addition product **18** with trihydroxyphenylboronate (**2**) was slightly lower ($\Delta\Delta G^\ddagger = 2.6 \text{ kcal/mol}$) in energy than the reaction of palladium hydroxide complex **19** with **1**, suggesting that both paths are capable of forming Pd–O–B linkages. However, the displacement of bromide with hydroxide from complex **18** was found to have a transition-state barrier of 18.6 kcal/mol, which suggests that Path A is more favorable than Path B (**Figure 3**).²¹ Moreover, the impact of phosphine

ligand on the transmetalation event has been computationally studied in depth by Lloyd-Jones and Harvey using $t\text{-Bu}_3\text{P}$, $(\text{CF}_3)_3\text{P}$, $(\text{CH}_3)_3\text{P}$, and Ph_3P . In this investigation, the steric parameters were found to be twice as important as the electronic parameters in the transmetalation event.²²

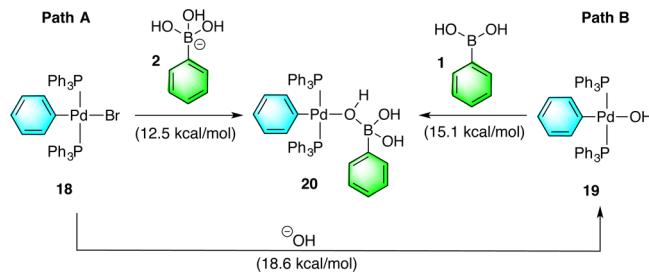
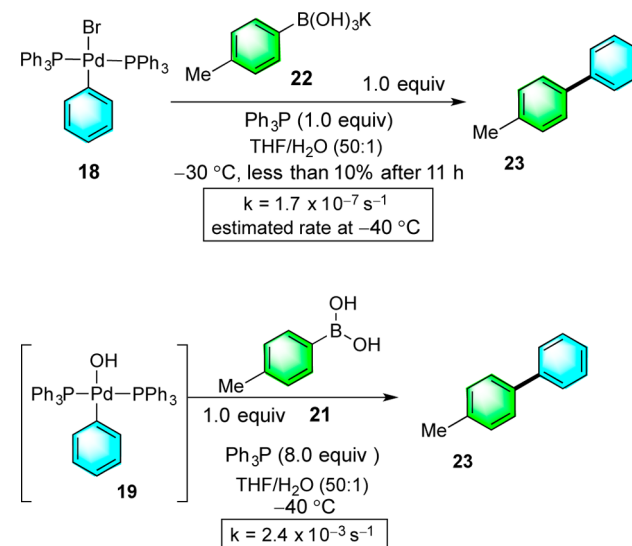


Figure 3. DFT-calculated values for transmetalation.

2.1.3. Experimental Studies. Understanding the role of hydroxide in the formation of the “missing link” **iii** (i.e., Path A or Path B) has inspired many investigations by Soderquist,¹⁹ Hartwig,²³ Amatore and Jutand,²⁴ and Schmidt.²⁵ By performing stoichiometric reactions of preformed $(\text{Ph}_3\text{P})_2\text{PdPhBr}$ (**18**) and $(\text{Ph}_3\text{P})_2\text{PdPhOH}$ (**19**) with **22** and **21** respectively, Hartwig’s group established that Path B is favored over Path A kinetically by more than 4 orders of magnitude (**Scheme 5**).

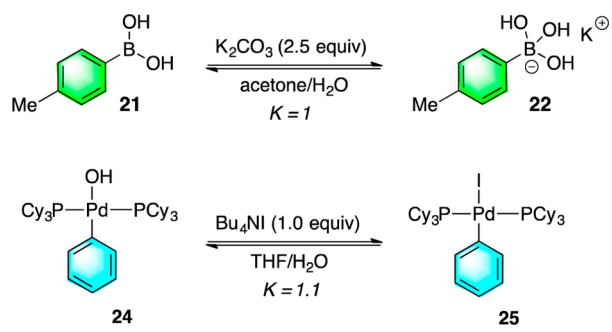
Scheme 5



Moreover, they established that the equilibrium population of 4-methylphenylboronic acid (**21**) and potassium 4-methylphenyltrihydroxyboronate (**22**) in acetone/H₂O in the presence of 2.5 equiv of K_2CO_3 is ca. 1:1. Interestingly, the relative populations of *trans*-($\text{Cy}_3\text{P})_2(\text{C}_6\text{H}_5)\text{Pd}(\text{OH})$ (**24**) and *trans*-($\text{Cy}_3\text{P})_2(\text{C}_6\text{H}_5)\text{Pd(I)}$ (**5**) are also approximately equal under simulated catalytic reaction conditions (**Scheme 6**). This conclusion was reinforced by extensive kinetic studies by Amatore and Jutand, who also identified multiple antagonistic roles for hydroxide ion. Although kinetic studies have provided evidence for these pathways, the actual composition and structure of the Pd–O–B-containing species have not been determined.

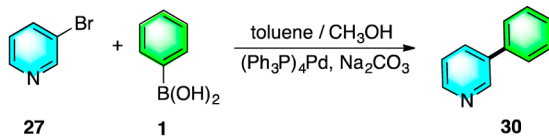
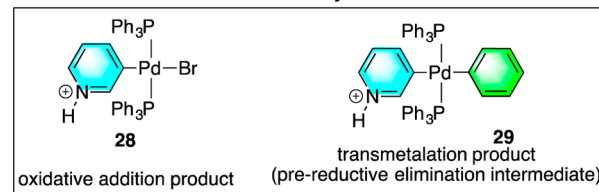
2.1.4. Attempts To Detect Reactive Intermediates. To observe pre-transmetalation intermediates, Canary and co-

Scheme 6



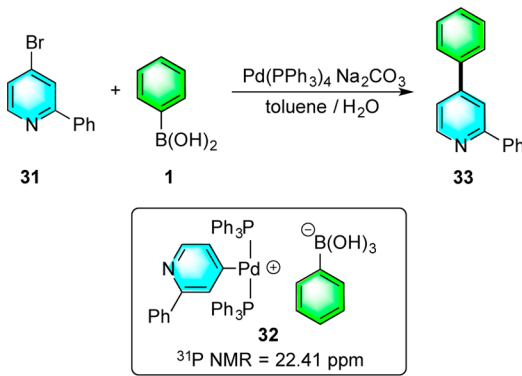
workers used electrospray mass spectrometry (ESI-MS) to probe the catalytic reaction between phenylboronic acid (**1**) and 3-bromopyridine (**27**) in toluene using $(Ph_3P)_4Pd$ and sodium carbonate as the base.²⁷ During the course of these experiments, both $[(pyrH)(Br)Pd(Ph_3P)_2]^+$ (**28**) and $[(pyrH)-(Ph)Pd(Ph_3P)_2]^+$ (**29**) are detected. The observation of the oxidative addition intermediate **28** and transmetalation product **29** clearly demonstrates how difficult it is to investigate the transmetalation step of the catalytic process (Scheme 7).

Scheme 7

*Observed by ESI*

Cid and co-workers' investigation on the transmetalation step of the Suzuki–Miyaura reaction involved the use of ³¹P NMR spectroscopy and computational methods.^{21a} The authors combined 4-bromo-2-phenylpyridine (**31**) and phenylboronic acid (**1**) with $(Ph_3P)_4Pd$ and were able to observe a ³¹P NMR signal at 22.41 ppm, which was assigned to $(Ph_3P)_2PdAr^-[(HO)_3BAr]$ (**32**) (Scheme 8). The predicted structure is

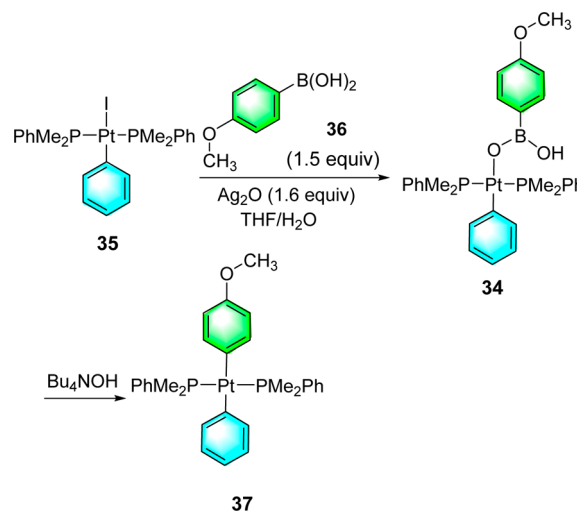
Scheme 8



based solely on DFT calculations. Although a new peak is observed by ³¹P NMR spectroscopy, no further structure determination was performed, thus precluding an assignment.

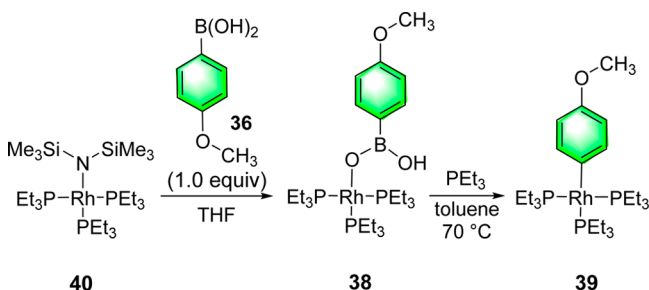
2.2. Formation of Related M–O–X Complexes. The transmetalation of arylboronic acids with complexes of late transition metals such as Pd, Rh, and Pt has been postulated in cross-coupling reactions as well as conjugate addition reactions. However, the intermediates involved in the transmetalation steps have rarely been observed for these processes. To date, stable Pt and Rh complexes of arylboronic acids have been characterized by single-crystal X-ray diffraction analysis. For example, Osakada²⁸ prepared Pt–O–B compound **34** by combining $(Me_3Ph)_2Pt(I)Ph$ (**35**) and 4-methoxyphenylboronic acid (**36**) with Ag_2O . Complex **34** is stable in THF until base is added, which induces transmetalation to the diarylpalladium intermediate **37** (Scheme 9).

Scheme 9



A similar Rh–O–B complex **38** prepared by Hartwig undergoes transmetalation to form $(Et_3P)_3Rh(C_6H_4OMe)$ (**39**) when heated to 70 °C (Scheme 10).²⁹ Interestingly, the Rh–O–B complex is proposed to undergo transmetalation without prior activation of the boron center.

Scheme 10



A related study from these laboratories on the transmetalation step in the Hiyama–Denmark cross-coupling process described the isolation and single-crystal X-ray diffraction analysis of several compounds containing Pd–O–Si linkages. These complexes enabled a systematic study on the requirements for the transfer of the organic group from silicon to palladium for both neutral (8-Si-4) and anionic (10-Si-5)

pathways.^{12b} These conclusions contradicted the paradigm that organosilicon compounds *must* be anionically activated to participate in the transmetalation processes. In general, arylsilanlates require anionic activation and react via 10-Si-5 intermediate **41**, whereas alkenylsilanlates undergo transmetalation directly from 8-Si-4 intermediate **42** (Figure 4). The ability to perform a similar study with Pd–O–B linkages would be ideal; however, the high propensity for transmetalation at room temperature makes their isolation and characterization difficult in practice.

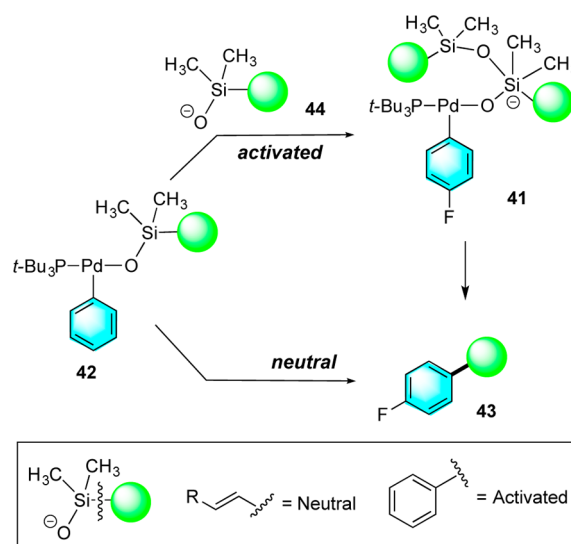


Figure 4. Hiyama–Denmark transmetalation pathways.

2.3. Rapid Injection NMR. Because of the apparently transient nature of species containing Pd–O–B linkages, routine methods such as ESI-MS and NMR spectroscopy are often unable to identify and characterize these highly reactive intermediates. Clearly, fast and low-temperature techniques are required to probe the mechanism of this crucial transmetalation step in the Suzuki–Miyaura reaction, as low barriers ($\Delta G^\ddagger = 14\text{--}22 \text{ kcal/mol}$) to transmetalation have been calculated.^{20\text{--}22} One such technique that has proven invaluable in similar mechanistic studies is rapid injection nuclear magnetic resonance spectroscopy (RI-NMR).³⁰ RI-NMR is a conceptually simple technique that was developed by McGarrity and co-workers in 1981 for the observation and characterization of reactive intermediates with short lifetimes.³¹ In practical terms, an RI-NMR experiment involves charging a substrate, typically the more sensitive compound, in an NMR tube spinning in the probe of an NMR spectrometer. Next, a calibrated syringe assembly is lowered into the magnet to allow for temperature equilibration, shimming, locking, etc., which are then followed by the injection of another reagent. Acquisition begins simultaneously with injection, which allows for rapid data collection. From the integration of the signals, the quantification of each species in solution can be performed with an internal standard. As a result, detailed quantitative kinetic data can be accessed even for fleeting intermediates. If pre-transmetalation intermediates could be generated and characterized by this method, it would provide the first opportunity to interrogate structure and reactivity relationships of this crucial step.

2.4. Goals of this Study. The aim of this project is to provide a complete understanding for the mechanism of the

Suzuki–Miyaura reaction by probing the pre-transmetalation intermediate by low-temperature and RI-NMR spectroscopy along with computational analysis. Specific goals include (1) full characterization of reaction intermediates such as the pre-transmetalation species **4**, (2) validation of structure of the proposed intermediates through independent synthesis, (3) demonstration of the kinetic competence of the characterized species containing Pd–O–B linkages to form cross-coupling product, and (4) quantum mechanical simulation of the transmetalation process involving these intermediates by computational modeling.³²

3. RESULTS AND DISCUSSION

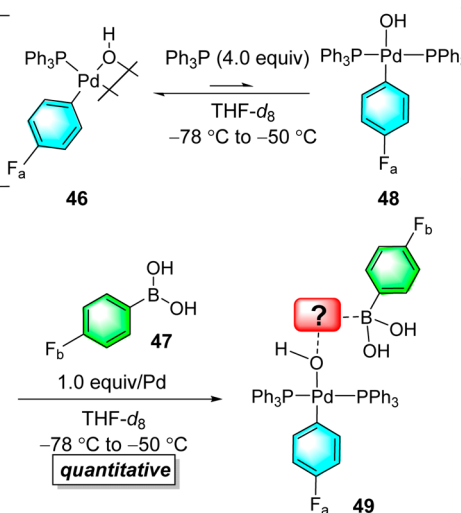
3.1. Preparation and Structural Analysis of Pd–O–B Complexes.

3.1.1. Preliminary Investigations of *trans*-(Ph_3P)₂(4-FC₆H₄)Pd(OH) with 4-Fluorophenylboronic Acid. Previous investigations that employed palladium complex [$(\text{Ph}_3\text{P})(\text{C}_6\text{H}_5)\text{Pd}(\text{OH})$]₂ as described above directed our preliminary studies to the use of fluorine-labeled derivatives [$(\text{Ph}_3\text{P})(4\text{-FC}_6\text{H}_4)\text{Pd}(\text{OH})$]₂ (**46**) and 4-fluorophenylboronic acid (**47**)³³ using ¹⁹F and ³¹P NMR spectroscopy.³⁴

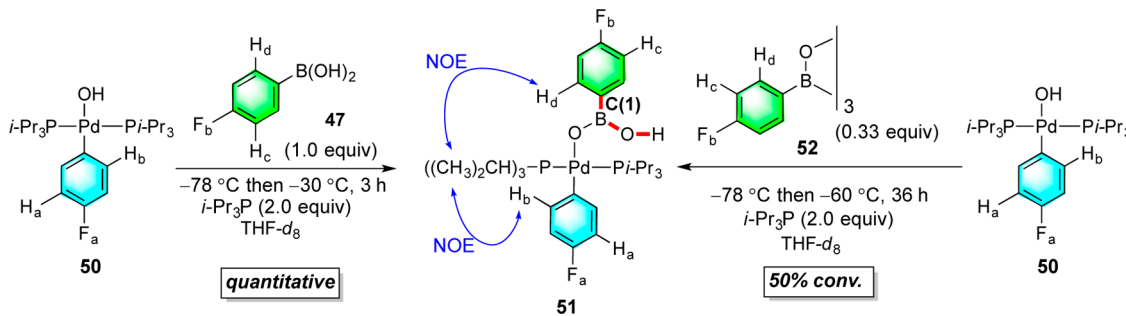
Addition of 4.0 equiv of Ph_3P to a THF solution of dinuclear complex **46** resulted in only trace conversion to *trans*-(Ph_3P)₂(4-FC₆H₄)Pd(OH) (**48**), indicating a thermodynamic preference for the Pd–(μ -OH)–Pd moiety (Scheme 11).³⁵ However, the addition of 4-fluorophenylboronic acid (1.0 equiv/Pd in **46**) to this solution at -50°C resulted in the observation of a new complex by ³¹P and ¹⁹F NMR spectroscopy. Interestingly, the ³¹P NMR spectrum displayed two singlets at -6.5 ppm (free Ph_3P) and 20.60 ppm in a ratio of 1:1, implying that the complex contained two molecules of Ph_3P based on the initial stoichiometry of starting materials. The ¹⁹F NMR spectrum displayed a new set of signals at -116.74 and -125.40 ppm in a 1:1 ratio. The observation of two ¹⁹F NMR resonances excluded the assignment of the new species as the product of transmetalation, *trans*-(Ph_3P)₂(4-FC₆H₄)Pd (which should appear as a single resonance), and was consistent with the assignment of an unsymmetrical species containing a Pd–O–B linkage such as **49**.

However, the complexity of the aromatic region in the ¹H and ¹³C NMR spectra prohibited assignments, thus making it impossible to unambiguously identify the structure of the new

Scheme 11

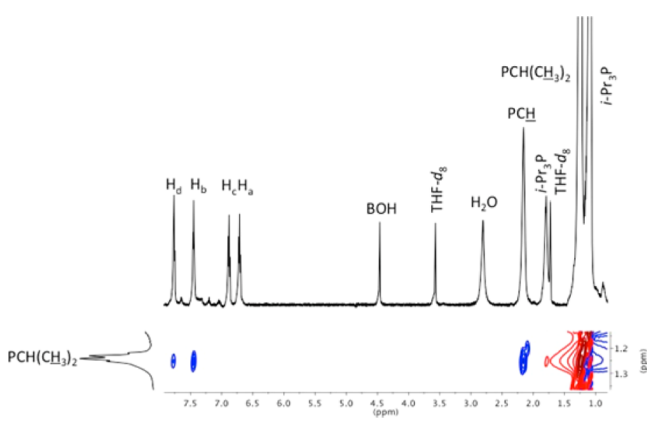


Scheme 12



species. Therefore, to clear the aromatic region of interfering signals, the Ph₃P ligand was replaced with a trialkylphosphine, *i*-Pr₃P, which readily forms stable mononuclear bis-phosphine palladium hydroxide complexes such as *trans*-(*i*-Pr₃P)₂(4-FC₆H₄)Pd(OH) (**50**).³⁵ Thus, our efforts switched to the study of mononuclear bis-phosphine palladium complexes to identify the key intermediate.

3.1.2. Reaction of *trans*-(*i*-Pr₃P)₂(4-FC₆H₄)Pd(OH) with 4-Fluorophenylboronic Acid and 4-Fluorophenylboroxine. Combination of *trans*-(*i*-Pr₃P)₂(4-FC₆H₄)Pd(OH) (**50**) and arylboronic acid **47** with 2.0 equiv of *i*-Pr₃P³⁶ in THF-*d*₈ at -78 °C, followed by warming to -60 °C, did not result in the formation of a new intermediate. Upon warming the solution at -30 °C for 3 h, quantitative conversion to a new discrete species was observed (Scheme 12, left). The bonding connectivity of the new species was established by the observation of strong, through-space interactions between aryl protons H_b and H_d with the methyl hydrogens on the *i*-Pr₃P group in the NOESY spectrum. This interaction reveals that both aryl residues were proximal to the phosphines and thus establishes the presence of a Pd–O–B linkage (Figure 5). The identity of the carbon bound to the boron atom C(1) was revealed in the HMBC (¹H–¹³C) spectrum by the observation of cross peaks between the BOH hydrogen with a single ¹³C signal at 138.68 ppm (red bonds).

Figure 5. NOESY spectrum of complex **51**.

The coordination geometry at the palladium atom was established by the appearance of the ¹³C NMR signal of the isopropyl methine carbon (PCH) at 25.38 ppm as an apparent triplet ($J_{P-C} = 10$ Hz) owing to virtual coupling,³⁷ along with a solitary ³¹P NMR signal at 29.98 ppm. These data indicate a *trans* arrangement of phosphine ligands bound to palladium. The valence state at boron was established by the observation

of a ¹¹B NMR signal at 29 ppm, indicating a tri-coordinate geometry (6-B-3)³⁸ that was also seen in the Pt²⁸ and Rh²⁹ complexes, **34** and **38**, mentioned above.

Support for the structural assignment of complex **51** was provided by an independent preparation from 4-fluorophenylboroxine (**52**) (0.33 equiv) and complex **50** with 2.0 equiv of *i*-Pr₃P in THF-*d*₈ at -78 °C, followed by warming to -60 °C. Under these conditions, a ca. 50% conversion to complex **51** was observed, with the remainder forming 4,4'-difluorobiphenyl cross-coupling product **53** (Scheme 12, right). The similarity of the spectroscopic data from these two independent syntheses, including the NOE cross peaks and ¹¹B NMR chemical shifts, provides compelling support for the structural assignment of **51** as a 6-B-3 palladium(II) complex containing a Pd–O–B linkage.

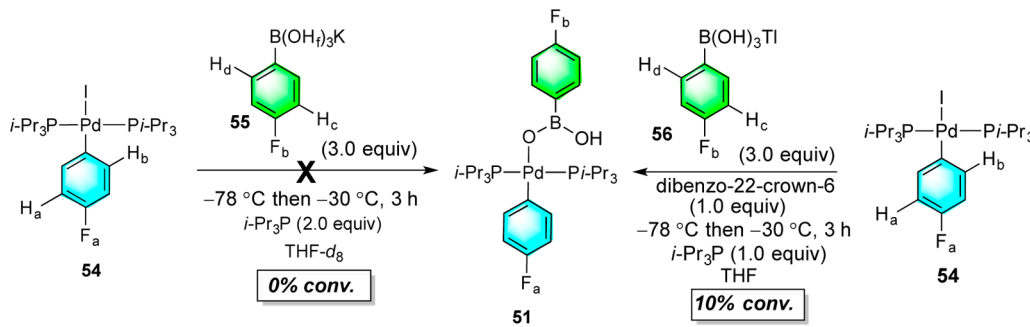
3.1.3. Reaction of *trans*-(*i*-Pr₃P)₂(4-FC₆H₄)Pd(I) with 4-Fluorophenylboronate Salts. An alternative preparation of the intermediate involves the direct displacement of halide from the bis-phosphine-ligated oxidative addition product, *trans*-(*i*-Pr₃P)₂(4-FC₆H₄)Pd(I) (**54**).³² However, treatment of a THF solution of complex **54** with 3.0 equiv of potassium 4-fluorophenylboronate (**55**) at -30 °C in THF with 2.0 equiv of *i*-Pr₃P resulted in no reaction (Scheme 13, left). Even upon warming to 30 °C, no cross-coupling product **53** was observed. The lack of reaction is most likely due to the steric hindrance at the palladium center provided by the bulky phosphine ligands, as well as the low solubility of **55** in THF.

To activate the palladium center toward nucleophilic attack, **54** was combined with 3.0 equiv of thallium 4-fluorophenylboronate (**56**) containing 1.0 equiv of *i*-Pr₃P and dibenzo-22-crown-6³⁹ to facilitate halide abstraction (Scheme 13, right). Although only a 10% conversion to **51** was observed by ¹⁹F and ³¹P NMR spectroscopy, the experiment demonstrated that intermediate **51** could be formed directly from complex **54**.

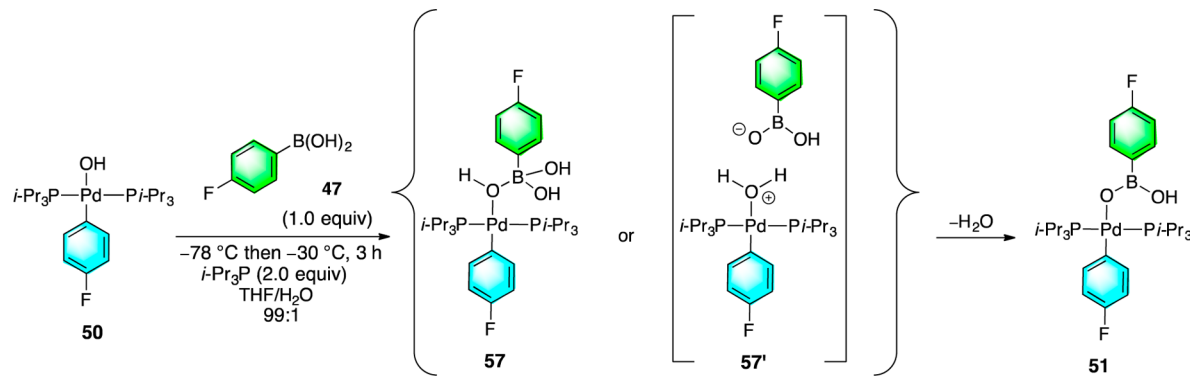
3.1.4. Attempts To Generate an 8-B-4 Complex from **51.** The formation of 6-B-3 complex **51** may arise either from a kinetically generated 8-B-4 complex **57** followed by rapid elimination of a single molecule of water or from displacement of a molecule of water from ion pair **57'**, which may be generated by protonation of complex **50** by boronic acid **47** (Scheme 14).⁴⁰ Because these experiments were performed in anhydrous THF, it is conceivable that the 8-B-4 complex **57** is thermodynamically unstable. Thus, a number of attempts to add water back were undertaken, beginning with generating **51** in THF/H₂O (99:1) mixtures; however, no changes in the ³¹P, ¹⁹F, or ¹¹B NMR spectra were observed at -30 °C (Scheme 14).

Next, the use of CsOH·H₂O was explored by combining 6-B-3 complex **51** (from **50** and **47**, *vide supra*) in THF at -78 °C

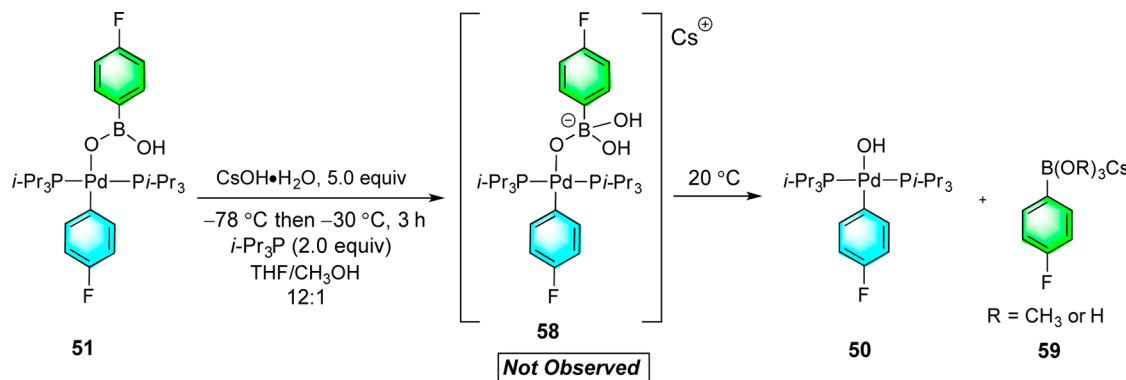
Scheme 13



Scheme 14



Scheme 15



with a solution of $CsOH \cdot H_2O$ (5.0 equiv) in methanol. The sample was monitored at $-30^{\circ}C$, but no changes in the ^{19}F , ^{31}P , or ^{11}B NMR spectra were observed. However, after the sample was warmed in 10 °C intervals up to 20 °C, cesium 4-fluorophenylboronate 59 and complex 50 were observed by ^{19}F and ^{31}P NMR spectroscopy, indicating that the arylboronic acid had been displaced from the palladium center (Scheme 15). This experiment supported the notion that arylboronate complexes such as 57 and 58 are indeed unstable. The reason for their instability was revealed by thermochemical calculations as detailed below.

3.1.5. Thermochemical Calculations on 6-B-3 and 8-B-4 Complexes. To gain further insight into the lack of stability of 8-B-4 complex 57, ground-state equilibrium energies were calculated using M06-2X/6-31G(d) on B3LYP/6-31(d)-optimized structures with a THF continuum solvent field. The loss of water from an initially formed 8-B-4 complex 57, yielding 6-B-3 complex 51, was found to be highly exergonic ($\Delta G^\circ = -10.8$ kcal/mol).

Surprisingly, the entropic advantage ($\Delta S^\circ = 0.048$ kcal/(mol·K)) is not offset by the expected enthalpic disadvantage of creating a coordinatively unsaturated boron ($\Delta H^\circ = 1.0$ kcal/mol) (Figure 6).

Inspection of space-filling models of 57 reveals that the OH groups on boron penetrate the van der Waals radii of the isopropyl methyl groups on phosphorus, thus destabilizing the four-coordinate geometry. Therefore, the instability of 57 is not related to the medium, but rather to the bulk of the two $i\text{-Pr}_3P$ groups attached to palladium. The solution to this problem then became obvious: remove a phosphine ligand from the complex. Indeed, calculation of the ground-state energies for monoligated complexes 60 and 61 reversed the equilibrium position, now substantially favoring the 8-B-4 complex ($\Delta G^\circ = -6.9$ kcal/mol) despite an unfavorable entropy ($\Delta S^\circ = -0.045$ kcal/(mol·K)). This preference is driven by the overwhelming enthalpic benefit of saturating the valences on boron ($\Delta H^\circ = -17.9$ kcal/mol). Accordingly, the focus of the investigation

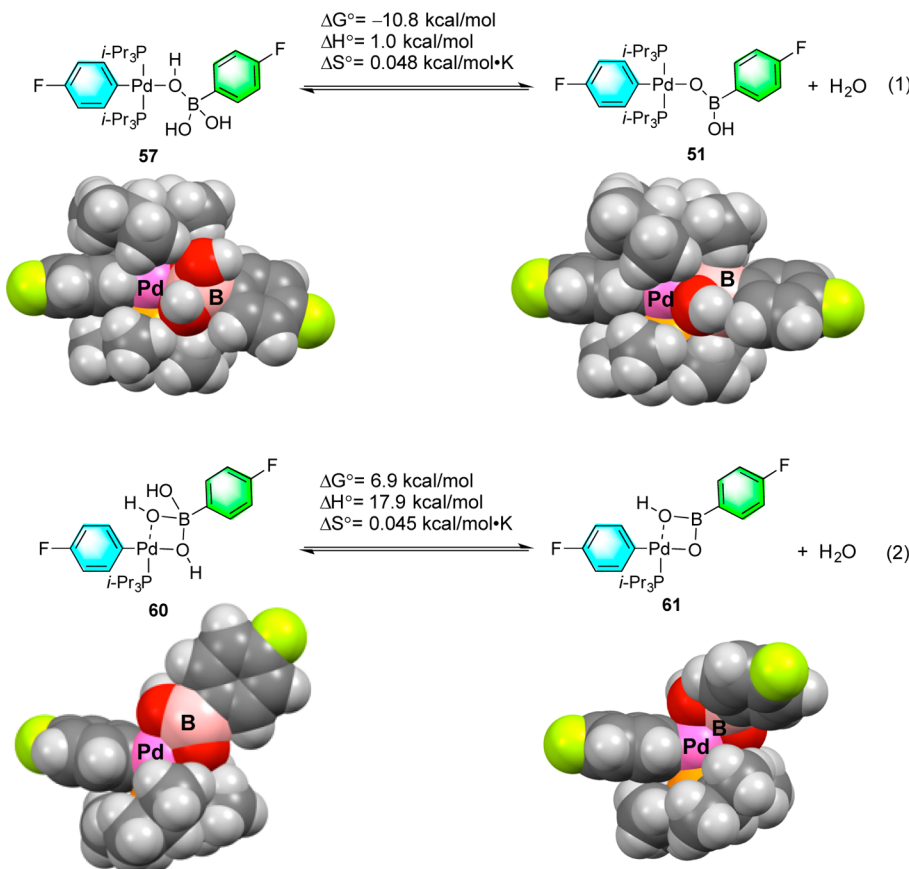
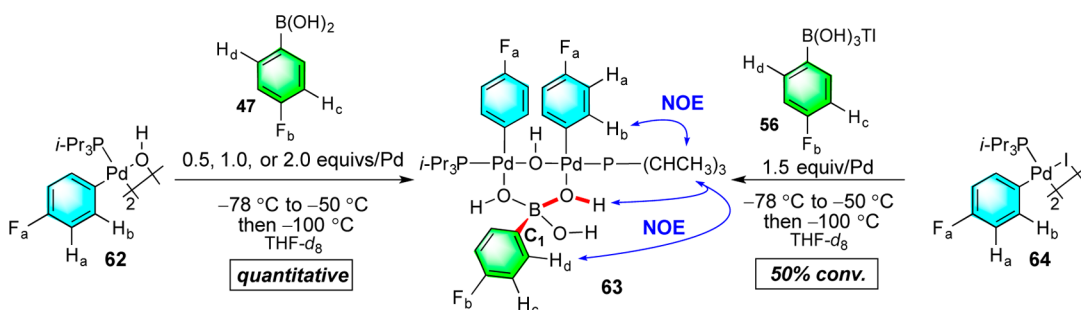


Figure 6. Calculated equilibria for loss of water at -30°C from 8-B-4 species **57** and **60**.

Scheme 16



switched to the study of monoligated arylpalladium(II) complexes to enable the generation of the long-sought 8-B-4 activated adduct.

3.1.6. Reaction of $[(i\text{-Pr}_3\text{P})(4\text{-FC}_6\text{H}_4)\text{Pd}(\text{OH})]_2$ with 4-Fluorophenylboronic Acid. Addition of a THF solution of **47** (1.0 equiv/Pd) to dimeric complex $[(i\text{-Pr}_3\text{P})(4\text{-FC}_6\text{H}_4)\text{Pd}(\text{OH})]_2$ (**62**)⁴¹ in THF-*d*₈ at -78°C , followed by warming to -50°C , resulted in no change in the ¹H NMR spectrum (Scheme 16). However, the ¹⁹F NMR spectrum displayed a sharp signal for F_a at -123.35 ppm but an extremely broadened signal for F_b at approximately -111.98 ppm , signifying a dynamic process. Upon cooling the solution to -100°C , new signals appeared in the aromatic region of the ¹H NMR spectrum, along with complete loss of the signals of **62**, but surprisingly with 50% of **47** remaining (Scheme 16, left). The incomplete consumption of the boronic acid could be interpreted as an unfavorable equilibrium or a different stoichiometry of complexation. The former interpretation was

eliminated by the addition of 2.0 equiv/Pd of **47** to complex **62**, whereupon no further incorporation of the arylboronic acid was observed. The connectivity in complex **63** was established by the observation of 1D-NOE, positive cross peaks between H_b, H_d, and the bridging OH group with the methyl hydrogens on the *i*-Pr₃P group. The observation of *positive* NOE cross peaks indicates slow molecular movements (tumbling) consistent with the larger molecular size of the 2:1 complex. Moreover, the resonances for H_b and for the methyl hydrogens on the *i*-Pr₃P group were exceptionally broadened at -100°C , indicating an observable barrier to rotation about both the P-Pd and aryl-Pd bonds. On the basis of the available data, the structure of this complex was assigned as the bridged bis-arylpalladium arylboronate complex **63**, which represents direct insertion of **47** into the dimeric complex **62** without further dissociation.⁴²

The unexpected 2:1 stoichiometry of complex **63** was confirmed by combining a THF-*d*₈ solution of **47** (0.5 equiv/

Pd) with a THF-*d*₈ solution of **62** at -60 °C, followed by cooling to -100 °C, whereupon a quantitative conversion to **63** was observed. The ¹¹B NMR spectrum of complex **63** did not reveal a discrete signal, owing to the rapid exchange between the arylboronic acid **47** and the palladium hydroxide complex **62**, as confirmed by EXSY experiments.

3.1.7. Reaction of [(*i*-Pr₃P)(4-FC₆H₄)Pd(I)]₂ with Thallium 4-Fluorophenylboronate. To support the structural assignment of complex **63**, an independent synthesis was performed by combining 1.5 equiv/Pd of thallium arylboronate **56** with [(*i*-Pr₃P)(4-FC₆H₄)Pd(I)]₂ (**64**)³² in THF-*d*₈ at -78 °C, followed by warming to -50 °C. Upon cooling the mixture to -100 °C, the identity of complex **63** was confirmed in a 1:1 ratio with cross-coupling product **53** by ¹H, ¹⁹F, and ³¹P NMR spectroscopy, indicating the ability to form the Pd–O–B linkage in **63** with complex **64** directly (Scheme 16, right).⁴³

3.1.8. Variable-Temperature NMR Analysis of Complex 63. The activation energy of exchange between complex **63** and arylboronic acid **47** was measured by variable-temperature NMR spectroscopy. The ¹⁹F NMR spectra of a 1:1 ratio of complex **63** and unbound **47** were recorded over a course of multiple experiments at temperatures ranging from -100 to -10 °C in THF (Figure 7). The rapid exchange of **63** and

approximate coalescence temperature (*T*_c) was measured at -40 °C by the signals merging with the baseline. The rate constant *k*_c at coalescence was measured using $k_c = \pi\Delta\nu/\sqrt{2}$, where $\Delta\nu$ is the maximum chemical shift difference (1068 Hz) between **63** and **47** at -100 °C. Using the Eyring equation $\Delta G_e^\ddagger = -RT_c \ln(k_c h/k_B T_c)$, the activation of exchange was measured approximately as $\Delta G_e^\ddagger \approx 10$ kcal/mol. This low barrier of exchange between **63** and **47** suggests that the broad ¹¹B NMR signal is caused by rapid changes in the coordination state of boron.

3.1.9. Reaction of [(*t*-Bu₃P)(4-FC₆H₄)Pd(OH)]₂ with 4-Fluorophenylboronic Acid. In an attempt to form a complex with 1:1 Pd/B stoichiometry, the larger *t*-Bu₃P ligand was employed to weaken the Pd–(μ-OH)–Pd bonds and form a T-shaped palladium hydroxide complex. Thus, addition of a THF-*d*₈ solution of complex **65** to a THF-*d*₈ solution of **47** (1.0 equiv/Pd) at -78 °C, followed by warming to -60 °C, produced no new complexes. However, upon cooling the solution to -100 °C, a new complex emerged with complete consumption of **67**, with 1.0 equiv of **47** remaining (Scheme 17). The structure of this complex was assigned as the bridged bis-arylpalladium arylboronate complex **67**, by analogy to complex **63**. Two discrete H_b signals were observed at -100 °C, wherein the barrier to rotation about the palladium aryl bond was found to be ~9 kcal/mol.⁴⁴ Thus, even the bulkier *t*-Bu₃P ligand could not effect dissociation of the 2:1 complex.

3.1.10. Reaction of [(*i*-Pr₃P)(4-FC₆H₄)Pd(OH)]₂ with 4-Fluorophenylboronic Acid in THF/CH₃OH. The surprising formation of 2:1 complex **63** raised a number of questions regarding the origin of its stability. Because this structure is heavily dependent upon the bridging capability of various oxygen atoms, it seemed logical to examine the effect of other donors on the stability of this complex.

Injection of CH₃OH⁴⁵ (60 μL) into a THF-*d*₈ solution of **63** with 1.0 equiv of **47** (from **62** and **47**, *vide supra*) at -55 °C resulted in the quantitative formation of a new species, **68** (Scheme 18, left). Attempts to confirm the incorporation of methanol into complex **68** by NMR spectroscopy were unsuccessful, most likely because of rapid exchange with free methanol in solution. Therefore, the identity of complex **68** was verified by the reaction of 1.0 equiv/Pd 4-fluorophenyldimethoxyboronate **69** with palladium dimer **62** at -78 °C in THF-*d*₈/CD₃OD, followed by warming to -55 °C, whereupon a quantitative formation of complex **68** was observed by ¹H and ¹³C NMR spectroscopy (Scheme 18, right). This experiment clearly demonstrates that methanol does not convert the starting binuclear arylpalladium hydroxide complex into a T-shaped complex but instead creates a more Lewis acidic boron

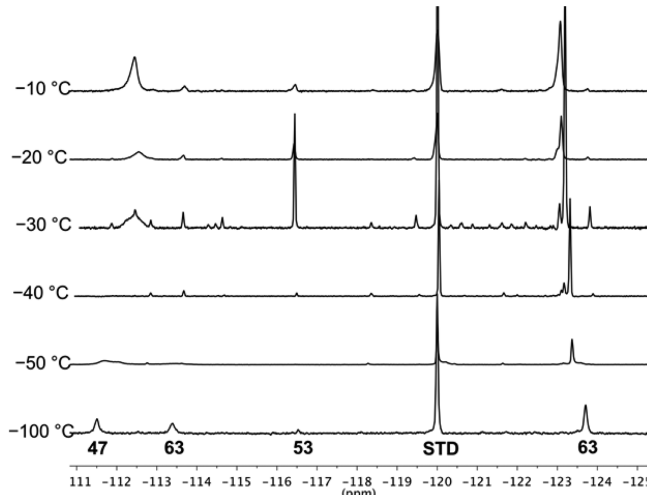
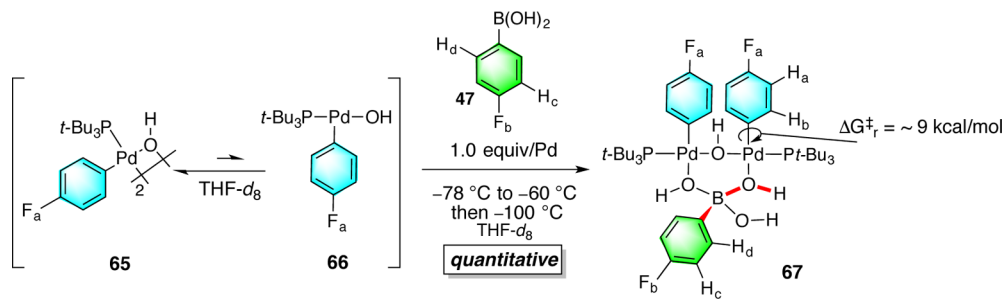


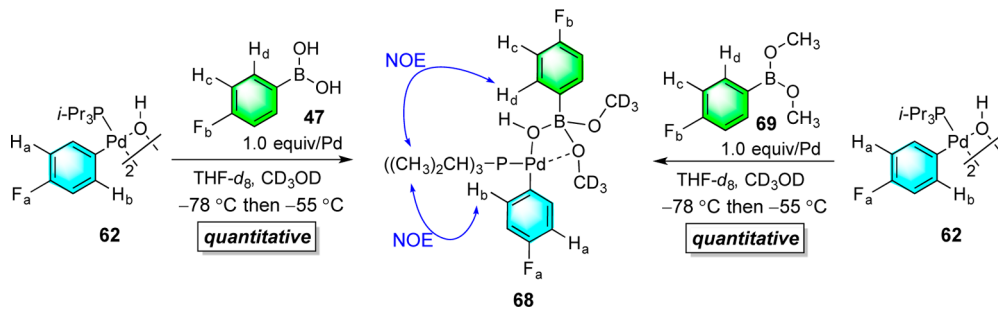
Figure 7. Stacked plot of ¹⁹F NMR spectra recorded for a THF solution of 1.0 equiv of **47** and 1.0 equiv of **63** over a range of temperatures (-100 to -10 °C) at 565 MHz.

unbound **47** is evidenced by the overlapping and broadening of their ¹⁹F NMR signals at higher temperatures (> -50 °C), and the slow exchange is evidenced at lower temperatures by the decoalescence of the ¹⁹F signals into well-resolved peaks. An

Scheme 17



Scheme 18

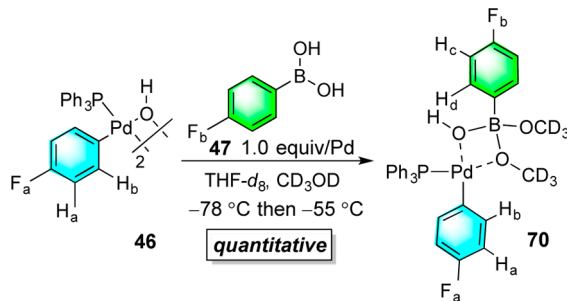


atom by replacing both hydroxyl groups with methoxy groups.⁴⁶

Nevertheless, the presence of a Pd–O–B linkage in **68** was established by the observation of cross peaks between the methyl hydrogens on the *i*-Pr₃P with both H_b and H_d using NOE spectroscopy. The ¹¹B NMR signal at 9 ppm was well within the chemical shift regime for tetra-coordinate boron (8–B-4) complexes.⁴⁷

3.1.11. Reaction of $[(Ph_3P)(4-FC_6H_4)Pd(OH)]_2$ with 4-Fluorophenylboronic Acid in THF/CH₃OH. To establish if similar 1:1 complexes can be formed with other ligands, $[(Ph_3P)(4-FC_6H_4)Pd(OH)]_2$ (**46**) was combined with 1.0 equiv/Pd of **47** at -78 °C in THF-*d*₈/CD₃OD, followed by warming to -55 °C. A new complex **70** was formed quantitatively, which displays spectroscopic characteristics similar to those of the other complexes (¹H, ¹³C, ¹⁹F, ³¹P, and ¹¹B NMR), and for which HMBC and HSQC experiments established connectivity (Scheme 19).

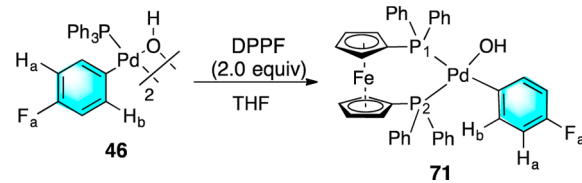
Scheme 19



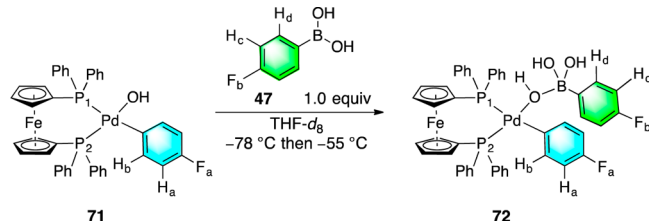
3.1.12. Reaction of $[(DPPF)(4-FC_6H_4)Pd(OH)]$ with 4-Fluorophenylboronic Acid in THF. The preference for a tri-coordinate boron atom in 6-B-3 complex **51** arose from the presence of two bulky *i*-Pr₃P ligands arranged in a *trans* configuration about the palladium (F- and B-strain).⁴⁸ It was of interest to investigate whether arranging the ligands in a *cis* coordination geometry would allow the boron atom to adopt a tetra-coordinate state. Therefore, following literature precedent,⁴⁹ (DPPF)(4-FC₆H₄)Pd(OH) was prepared by combining complex **46** with 2.0 equiv of DPPF in THF to form complex **71** (Scheme 20).

Next, complex **71** was combined with arylboronic acid **47** at -55 °C, which resulted in the quantitative conversion to a new species, **72** (Scheme 21). Complex **72** was characterized by ¹H, ³¹C, ¹⁹F, ¹¹B, and ³¹P NMR spectroscopy, with the HMBC (¹H–¹³C and ¹H–³¹P) and HSQC (¹H–³¹C) experiments establishing the connectivity.

Scheme 20



Scheme 21



At -55 °C, the assignment of the P(1) atom (11.47 ppm) in **72** was enabled by the observation of *trans* couplings across the Pd center to H_b (⁴J_{P-H}) and to H_a (⁵J_{P-H}), establishing a *trans* relationship between P(1) and the aryl group bound to palladium.⁵⁰ The ¹¹B NMR chemical shift was merged with the baseline, suggesting a rapid equilibrium between **72** and starting materials.⁵¹

3.2. Kinetic Analysis of the Complexes Containing Pd–O–B Linkages. The ability to generate pre-transmetalation intermediates with different coordination environments around both the boron and palladium atoms provided the opportunity to interrogate kinetic aspects of the transmetalation event. Specifically, the effect of ligand and organoboron source was probed by monitoring the decay of Pd–O–B-containing intermediates and formation of cross-coupling products by ¹⁹F NMR spectroscopy.

3.2.1. Kinetic Analysis of Complex **63 from $[(i-Pr_3P)(4-FC_6H_4)Pd(OH)]_2$ and 4-Fluorophenylboronic Acid.** Complex **63** was prepared as described in section 3.1.6 by the addition of a THF solution of **47** (1.0 equiv/Pd) to a THF solution of **62** at -78 °C. To establish the kinetic behavior, the sample was warmed to -30 °C, and the ¹⁹F NMR signals for both **53** and **63** were monitored. This analysis revealed a clean, first-order decay of the arylpalladium complex **63** and formation of **53** with $k_{obs} = (5.78 \pm 0.13) \times 10^{-4}$ and $(7.59 \pm 0.58) \times 10^{-4} \text{ s}^{-1}$, respectively. The similarity of rates for appearance of **53** and consumption of **63** suggests that transmetalation is the rate-determining step for this process.

The proposal that arylboronate complex **63** converts to **60** prior to transmetalation is supported by several lines of evidence.⁵² First, the kinetic behavior of arylpalladium complex

68 in THF/CH₃OH (a fully characterized 1:1 complex related to **60**) revealed a clean, first-order decay of **68** and formation of **53** with $k = (1.55 \pm 0.09) \times 10^{-3}$ and $(1.41 \pm 0.02) \times 10^{-3} \text{ s}^{-1}$, respectively. These values are very similar to the rates observed with complex **63** in THF. Moreover, the first-order behavior confirms that the transmetalation is an intramolecular process. Second, an Arrhenius analysis was performed by measuring the rates of formation of **53** (from **62** and 1.0 equiv/Pd of **47**) at four different temperatures ranging from -40 to -10 °C in THF. Upon plotting $\ln(k/T)$ vs T^{-1} , a linear slope was obtained, allowing the enthalpic ($\Delta H_{243.15}^\ddagger = 15.98 \pm 0.79 \text{ kcal/mol}$) and entropic ($\Delta S_{243.15}^\ddagger = -0.0069 \pm 0.0032 \text{ kcal/mol}$) activation parameters to be extracted using the Eyring equation. The similarity of the measured and calculated activation parameters (see section 3.3.1) strongly suggests that complex **63** rearranges to **60** prior to transmetalation (Table 1).

Table 1. Activation Parameters for the Transmetalation Step

entry	$\Delta G_{243.15}^\ddagger, \text{ kcal/mol}$	$\Delta H_{243.15}^\ddagger, \text{ kcal/mol}$	$\Delta S^\ddagger, \text{ kcal/mol-K}$
measured ^a	17.7 ± 1.1	15.98 ± 0.79	-0.0069 ± 0.0032
calculated	15.38	14.57	-0.003

^aAverage of triplicate runs.

3.2.2. Effect of Phosphine Ligand on the Rate of the Transmetalation Step. To establish the effect of phosphine ligand (DPPF, *i*-Pr₃P, Ph₃P) on the rate of transmetalation, complexes **71**, **62**, and **46** were combined separately with 4-fluorophenylboronic acid (**47**) (1.0 equiv/Pd) at -10 °C to generate **72**, **60**, and **73**, respectively, such that their ¹⁹F NMR signals could be monitored.⁵³ Each complex exhibited first-order decay, providing accurate values for k_{obs} (Table 2). The slower reaction rate of the DPPF-ligated complex compared to those of the Ph₃P- and *i*-Pr₃P-ligated complexes suggests that a ligand dissociation event takes place prior to the transmetalation event in complex **72**. The rate of transmetalation

Table 2. Effect of Phosphine Ligand on Rate^a

entry	complex	ligand	$k, 10^{-3} \text{ s}^{-1}$	k_{rel}
1	72	DPPF	2.75 ± 0.05	1.00
2	60	<i>i</i> -Pr ₃ P	8.09 ± 0.86	2.94
3	73	Ph ₃ P	9.95 ± 0.71	3.61

^aAverage of triplicate runs.

from the Ph₃P complex **73** was slightly faster than that from the *i*-Pr₃P complex **60**, indicating that the increased rate is not related to the size of the ligand, but rather to the electrophilicity of the palladium center.⁵⁴ From these data, the rate of the transmetalation process follows the trend Ph₃P > *i*-Pr₃P > DPPF, highlighting the need for generating a coordinatively unsaturated and electrophilic palladium atom during the transmetalation process.

3.2.3. Kinetic Analysis of 6-B-3 Complex **51.** Complex **51** (generated from **47** and **50**, see section 3.1.2) was thermally stable at -30 °C for more than 24 h in the presence of *i*-Pr₃P, indicating that a higher temperature would be needed to form cross-coupling product **53**. In fact, warming a THF solution of **51** to 20 °C resulted in the formation of **53**. However, it did not display the first-order behavior observed for the previous complexes, but rather exhibited S-shaped concentration vs time curves, indicating that the k_{obs} increases over the course of the reaction, which is characteristic of autocatalysis or an induction period. The kinetic order in phosphine was determined by monitoring the rate of decay of **51** in THF solutions containing increasing amounts of *i*-Pr₃P, ranging from 97 to 294 mM at 20 °C. The S-shaped kinetic profiles were fitted, and v_{max} was extracted from the data.⁵⁵ Plotting $\log[v_{\text{max}}]$ vs $\log[i\text{-Pr}_3\text{P}]$ provided a straight line with a slope of -1.01 ± 0.05 , consistent with an inverse dependence on phosphine (Table 3). This dependence indicates that a phosphine ligand must dissociate in a pre-equilibrium process that leads to putative 14-electron palladium complex **61** (Figure 8). The requirement for this dissociation event is supported by computational studies that reveal high barriers for direct transmetalation from intermediates such as **51**.²⁰

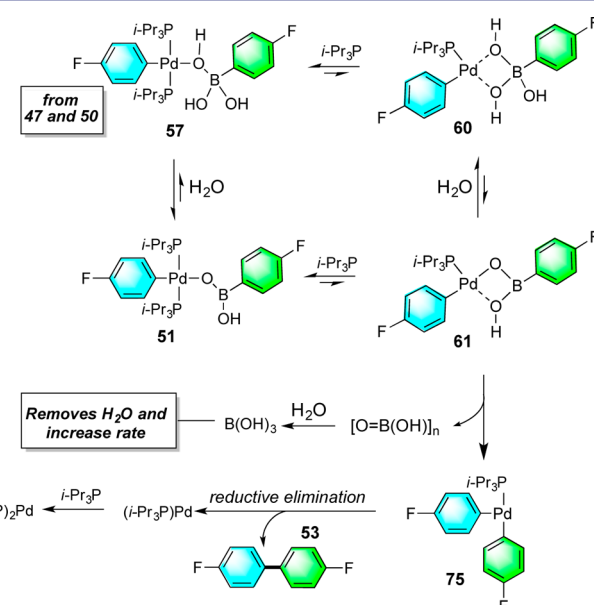


Figure 8. Proposed mechanism for cross-coupling formation from 6-B-3 complex **51**.

3.2.4. Probing the Transmetalation from 6-B-3 Complex **51: Autocatalysis Explained.** The S-shaped kinetic profiles observed for the reactions outlined above are indicative of an increase in rate during the reaction, which is likely the result of a product catalyzing its own formation. The stoichiometrically mandated products of this cross-coupling reaction are biaryl **53**, (*i*-Pr₃P)₂Pd, and boric acid. Because **53** is an inert organic

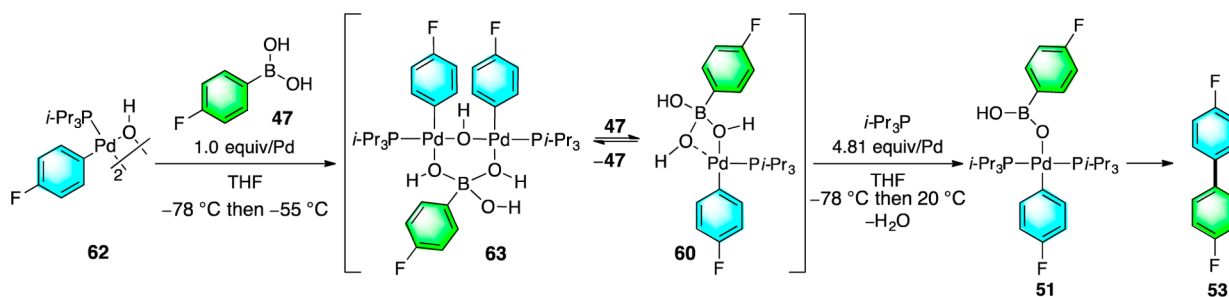
Table 3. Rates of Cross-Coupling Product **53** Formation from **51**^a

entry	amount of <i>i</i> -Pr ₃ P, equiv	additive	rate, ^a 10^{-3} mM s ⁻¹
1	2.85	—	4.48 ± 0.65
2	3.81	—	3.24 ± 0.12
3	5.41	—	2.42 ± 0.48
4	8.62	—	1.37 ± 0.96
5 ^b	3.81	(<i>i</i> -Pr ₃ P) ₂ Pd	2.86 ± 0.36
6 ^c	5.41	H ₂ O	1.11 ± 0.04
7 ^d	3.81	—	3.26 ± 0.17

^aAverage of triplicate runs. ^b0.25 equiv of (*i*-Pr₃P)₂Pd was added. ^c10 equiv of water was added. ^dComplex **51** was formed by the addition of *i*-Pr₃P to complex **73**.

compound, it is highly unlikely that it can serve as a catalyst. On the other hand, the initial palladium-containing byproduct, (*i*-Pr₃P)_nPd, is a more likely candidate for accelerating the process by scavenging *i*-Pr₃P from **51**. However, under the conditions of the kinetic measurements which employ an excess of *i*-Pr₃P (2.85–8.62 equiv/Pd), the Pd(0) species should already be saturated, thus precluding the possibility of autocatalysis. Interestingly, upon dissolving (*i*-Pr₃P)₃Pd in THF, both (*i*-Pr₃P)₂Pd and *i*-Pr₃P are observed, which means the palladium center cannot accept a third ligand in solution.⁵⁶ Not surprisingly, upon the addition of 0.25 equiv of (*i*-Pr₃P)₂Pd to a solution of **51** with 3.81 equiv of *i*-Pr₃P, S-shaped profiles were still observed with $v_{\max} = (2.86 \pm 0.36) \times 10^{-3}$ mM s⁻¹, which was within error of the v_{\max} ($3.24 \pm 0.12) \times 10^{-3}$ mM s⁻¹, obtained in the absence of the additive (Table 3, entry 5). The persistence of autocatalytic behavior confirms that no order dependence is observed for the Pd(0) byproducts during the reaction, leaving only the boric acid as the remaining culprit for the S-shaped profiles. Unfortunately, boric acid could not be tested because of its low solubility in THF, suggesting that no further options existed. However, inspection of Figure 8 reveals that, if transmetalation is occurring via **61**, boric acid is in fact not formed directly. Rather, the immediate byproduct of transmetalation is metaboric acid, which scavenges the water molecule generated during the formation of **51** to form boric acid. Thus, the role of water now becomes a factor worth investigating for the origin of autocatalysis.

Scheme 22

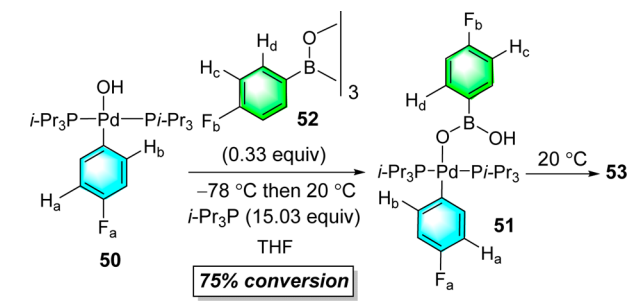


One reasonable hypothesis for the role of water is that it can bind to the boron atom in **61**, forming 8-B-4 species **60** (Figure 8), thus opening a second pathway that lowers the equilibrium concentration of **61**.⁵⁷ Despite the fact that **60** is itself kinetically competent for transmetalation (section 3.2.1), in the presence of excess *i*-Pr₃P this species rapidly reverses back to **51**, thus constituting a parasitic as opposed to a productive pathway. Moreover, if product formation were occurring via 8-B-4 complex **60**, then the highest rate should be observed at the beginning of the reaction because **60** would be at its highest concentration. To provide support for this hypothesis, it was necessary to demonstrate the ability to independently convert **60** to **51** in the presence of *i*-Pr₃P. Thus, a solution of complex **63** was prepared from **47** (1.0 equiv/Pd) and **62** in THF at -78 °C, followed by warming to -55 °C. As previously described, a mixture of **63** (which is in equilibrium with **60**) and 1.0 equiv of **47** was observed by ³¹P and ¹⁹F NMR analysis (Scheme 22). Upon addition of 60 μ L of a 1.6 M THF solution of *i*-Pr₃P at -78 °C to this solution, followed by warming to 20 °C, 6-B-3 complex **51** was observed, along with minor amounts of cross-coupling product **53**. The kinetic behavior of complex **51** generated by this route was found to have a v_{\max} matching that seen for the formation of **51** from **47** and **50** (Table 3, entries 2 and 7). Thus, it appears that water is in fact inhibiting the cross-coupling by shunting **61** to 8-B-4 intermediate **60**, which is captured by excess phosphine to arrive at resting state **51**.

Further support for the inhibitory role of water was obtained by monitoring the reaction of 6-B-3 complex **51** containing 5.41 equiv of *i*-Pr₃P and an additional 10.0 equiv of water. The v_{\max} was indeed found to be slower than with no additional water present (Table 3, entry 6). This observation suggests that, if complex **60** were being formed (from **61** and water), then it reverts to **51** by recombination with *i*-Pr₃P faster than it undergoes transmetalation at 20 °C. Finally, if the role of water is to inhibit the transmetalation via **61**, then generating **61** in the absence of water should remove the autocatalytic behavior.

In fact, the water-free preparation of **51** has already been described as part of the structural proof (Scheme 12) by combination of complex **50** and arylboroxine **52** (0.33 equiv) in THF. Repeating this procedure at -78 °C in the presence of 15.03 equiv of *i*-Pr₃P allowed the intrinsic reactivity of **51** to be determined (Scheme 23).⁵⁸ Clean first-order kinetic behavior was observed for decay of **51** ($(1.25 \pm 0.60) \times 10^{-4}$ s⁻¹) and formation of **53** ($(7.14 \pm 0.43) \times 10^{-5}$ s⁻¹) (Scheme 23). Thus, the observation of normal first-order kinetic behavior for **61** in the absence of water provides a compelling albeit unexpected explanation for the observation of autocatalysis. The equivalent of water generated from the combination of **47** and **50** (Figure 8) inhibits the transmetalation via **61** by redirecting this

Scheme 23



intermediate to 8-B-4 complex **60**, which is converted to resting state **51** in the presence of excess *i*-Pr₃P. However, as the reaction proceeds, the metabolic acid byproduct (BO(OH)) scavenges the water to form boric acid and consumes the inhibitor (water), thus accounting for the observed autocatalytic behavior (Figure 8). This observation also provides compelling evidence that a tri-coordinate boron species can undergo unassisted transmetalation.

3.3. Computational Analysis of the Reaction Profile for Complexes Containing Pd–O–B Linkages. To gain further insight into the transmetalation step, transition-state structures were calculated at the M06-2X/6-31G(d) level on B3LYP/6-31(d)-optimized structures with a THF continuum solvent field for the activated 8-B-4 complex **60**, along with unactivated 6-B-3 complex **61**. Our previous computational investigation of arylpalladium arylsilanolate complexes revealed

a significant difference in the energy profiles of isomeric arylpalladium complexes.^{12b} These three-coordinate species can exist in two configurations about palladium in which an empty site is either *trans* to the aryl group (*TA*) or *trans* to the phosphine (*TP*). For completeness, both isomers were calculated for all the ground states, intermediates, transition states, and products.

3.3.1. Computational Analysis of Complex **60.** The energy profile for the transmetalation event from 8-B-4 complex **60** is summarized in Figure 9. The experimentally observed ground-state structure **60-GS** has two bridging hydroxyl groups bound to the palladium atom; however, for the transmetalation event to take place, an empty coordination site is needed. The two bridging hydroxyl groups are nonequivalent: one is *trans* to the aryl group (red), and the other is *trans* to the phosphine (black). Cleavage of either of these groups will lead to their respective coordinatively unsaturated complexes described above, which are “*TA*” (*trans* to aryl, red) or “*TP*” (*trans* to phosphine, black). The energies of transition states **60-InterTS-TA** and **60-InterTS-TP** for the formation for the two different T-shaped complexes are 9.37 and 8.44 kcal/mol, respectively, whereas the energies of the resulting intermediates **60-Inter-TA** and **60-Inter-TP** are 8.93 and 5.13 kcal/mol, respectively. The principal factors contributing to these energies are the electronic and steric effects of the two different substituents, the aryl group and the phosphine. The electronic effect would weaken the bond to the red oxygen to a greater extent than that to the black oxygen because of the greater kinetic *trans* effect⁵⁹ of the aryl group compared to the phosphine, thus favoring **60-**

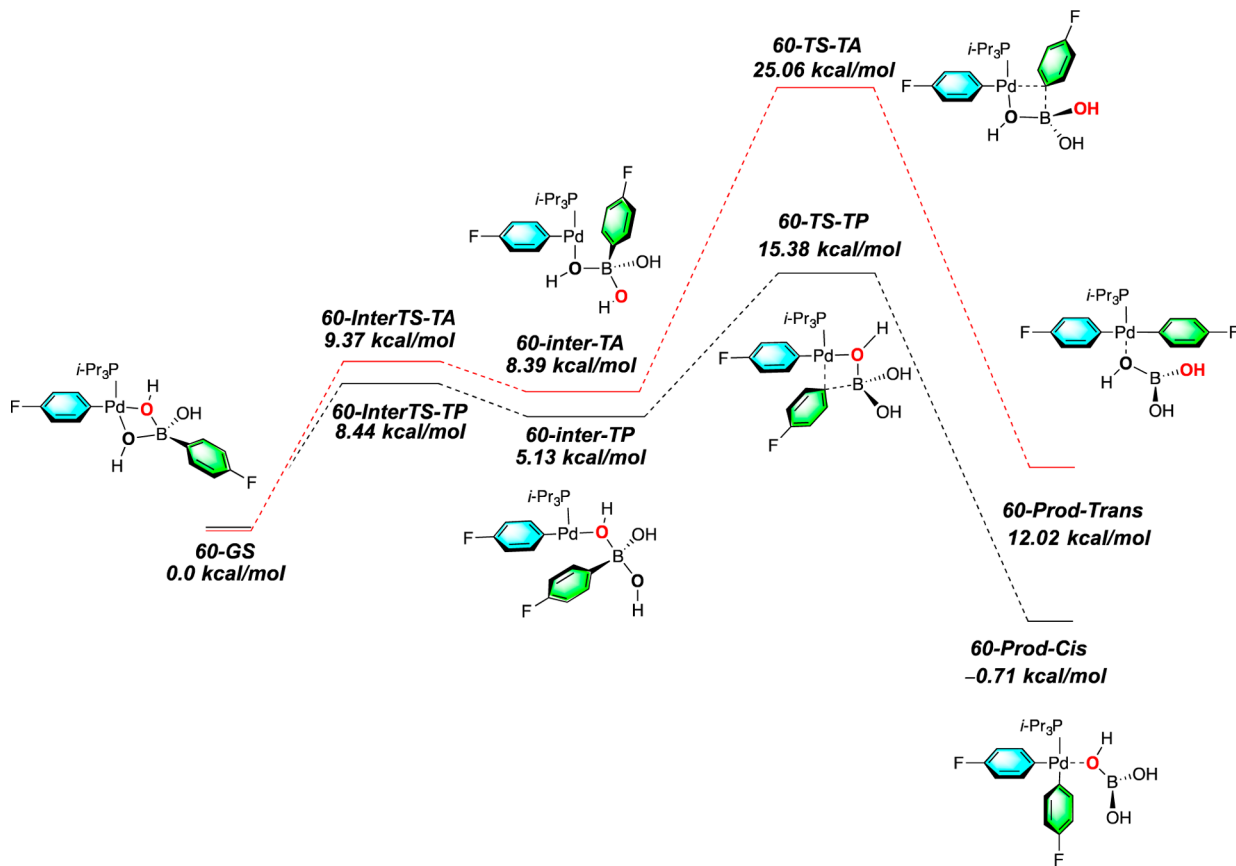


Figure 9. Energy profile for the transmetalation of **60**. Free energies are calculated using M062X/LANL2DZ-6-31G(d) with CPCM solvation modeling (solvent = THF) for single-point energies with thermal corrections from B3LYP/LANL2DZ-6-31G(d) at 243.15 K.

InterTS-TA. The steric contribution arises from interaction of the B-aryl group with those two substituents as it rotates toward the empty coordination site on the palladium in the transition state. Clearly, steric repulsion in **60-InterTS-TA** is greater as the B-aryl group becomes proximal to the bulky *i*-Pr₃P ligand. Thus, the difference of 0.93 kcal/mol favoring **60-InterTS-TP** suggests that the steric effect dominates in this process.⁶⁰ In fact, the dominance of this steric repulsion can be seen in the lower energy for all of the transition states and intermediates in the *TP* compared to the *TA* series.

In the critical transmetalation event, the activation energies for the B-aryl transfer for **60-TS-TA** and **60-TS-TP** are 25.06 and 15.38 kcal/mol, respectively, reflecting a remarkable activation energy difference of 9.7 kcal/mol. The greater activation barrier to B-aryl migration for **60-TS-TA** can be attributed to the significant steric congestion around the palladium atom caused by the presence of the bulky *i*-Pr₃P group, whereas migration of the B-aryl group to the empty coordination site in **60-TS-TP** is free of such repulsions and thus is energetically more favorable (Figure 10). These energetic differences are reflected in bonding distances between the palladium atom and the ipso carbon of the migrating aryl group, as shown in Figure 10. An additional electronic contribution comes from migration of the B-aryl group to the site opposite to the substituent with the stronger *trans* effect in **60-TS-TA**, thus constituting a kinetic deterrent. The activation barrier for the transmetalation transition state **60-TS-TP** (15.38 kcal/mol) is consistent with the experimentally measured value of 17.7 ± 1 kcal/mol (Table 2).⁶¹

After the transmetalation event, the immediate product is either **60-Prod-Trans** or **60-Prod-Cis** diarylpalladium complex with the coordinated B(OH)₃ *trans* to *i*-Pr₃P or the 4-

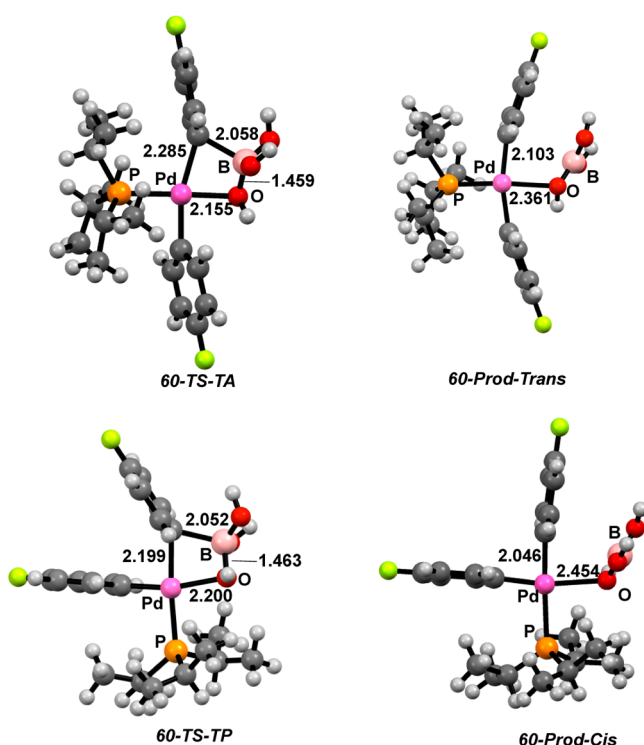


Figure 10. Energy profile for the transmetalation of **60**. Free energies are calculated using M062X/LANL2DZ-6-31G(d) with CPCM solvation modeling (solvent = THF) for single-point energies with thermal corrections from B3LYP/LANL2DZ-6-31G(d) at 243.15 K.

fluorophenyl group. The reductive elimination is presumably initiated by the dissociation of boric acid, thus generating the active tri-coordinate diarylpalladium complexes which are poised to form cross-coupling products.⁶²

3.3.2. Computational Analysis of Complex **61.** The energy surface calculated for the 6-B-3 complex **61** is shown in Figure 11. Inspection of the energy profile reveals that the ground states **61-React-TP** and **61-React-TA** differ by 0.99 kcal/mol. The energies of transition states **61-InterTS-TA** and **61-InterTS-TP** for the formation for the two different T-shaped complexes are 7.62 and 7.92 kcal/mol, respectively. The difference of 0.3 kcal/mol favoring **61-InterTS-TA** indicates that the kinetic *trans* effect⁵⁹ of the aryl group is now dominant compared to the steric repulsion engendered by the *i*-Pr₃P ligand.⁶³ However, in all succeeding steps on the energy profile, the structures in the *TA* family are of significantly higher energy than those in the *TP* family. This behavior can be understood in terms of the same steric and electronic influences as were seen in the 8-B-4 transition-state structures (Figure 11). After the transmetalation event, the diarylpalladium complexes (**61-Prod-Cis**, **61-Prod-Trans**) are only 0.78–1.13 kcal/mol downhill, thus indicating very late transition states.

The existence of late transition states is clearly signaled by the small difference in lengths of the forming bonds between the *ipso* carbon on the migrating group and the palladium atom for both **61-TS-TP** (2.085 Å) and **61-TS-TA** (2.171 Å) compared to **61-Prod-Cis** (2.069 Å) and **61-Prod-Trans** (2.154 Å), respectively. In this series the bonds are shortened by only 0.016–0.017 Å, whereas in the 8-B-4 series the corresponding changes for **60-TS-TP** (2.199 Å) and **60-TS-TA** (2.285 Å) compared to **60-Prod-Cis** (2.046 Å) and **60-Prod-Trans** (2.103 Å) are much larger (0.153–0.182 Å, Figures 10 and 12).

The subsequent reductive elimination is presumably initiated by the dissociation of the boron species to form free diarylpalladium complexes (*Pd-Prod-Cis*, *Pd-Prod-Trans*). However, the computational modeling of this event leads to a prohibitively endergonic process, which is most likely ascribable to the high energy of the O=B(OH) moiety. To solve this problem, we assume that some kind of bimolecular oligomerization takes place to remove O=B(OH) as a byproduct. Thus, to calculate the energies of the final reductive elimination products, instead of directly using the energy of O=B(OH), one-third energy of the O=B(OH) trimer, metaboric acid, was computed and added to the tri-coordinate diarylpalladium complexes, which in turn gives reasonable energies to both *Pd-Prod-Trans* (1.42 kcal/mol) and *Pd-Prod-Cis* (-10.31 kcal/mol).⁶⁴

4. CONCLUSIONS

The combination of low-temperature and rapid injection NMR spectroscopic analysis has allowed the unambiguous demonstration that Pd–O–B linkages form prior to the transmetalation event in the Suzuki–Miyaura cross-coupling reaction. Structures of the intermediates identified were assigned by NMR spectroscopy, with the NOE and HMBC experiments being crucial in determining the bonding connectivity. These structural assignments were supported by independent synthesis, which clearly demonstrated that, under certain reaction conditions, both Path A and Path B can lead to pre-transmetalation intermediates. The ability to form Pd–O–B linkages provided the unprecedented opportunity to probe the effect of the phosphine ligand on both structure and

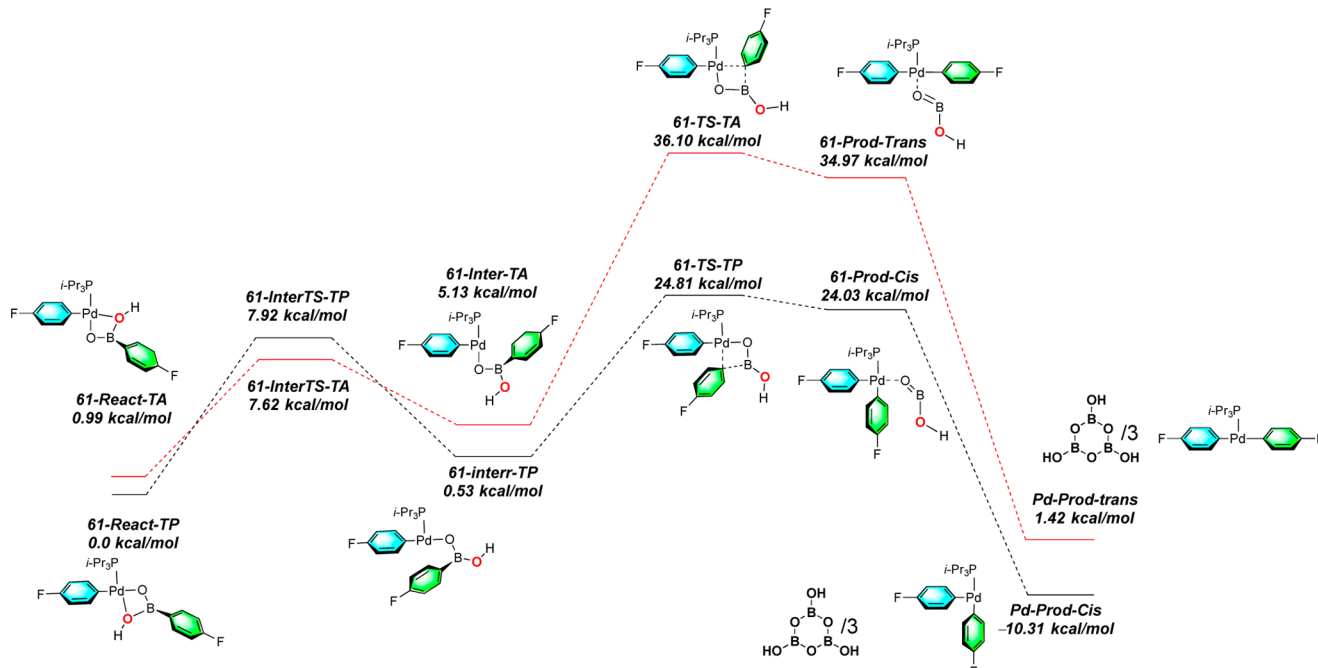


Figure 11. Energy profile for the transmetalation of 6-B-3 species **61**. Free energies are calculated using M062X/LANL2DZ-6-31G(d) with CPCM solvation modeling (solvent = THF) for single-point energies with thermal corrections from B3LYP/LANL2DZ-6-31G(d) at 243.15 K.

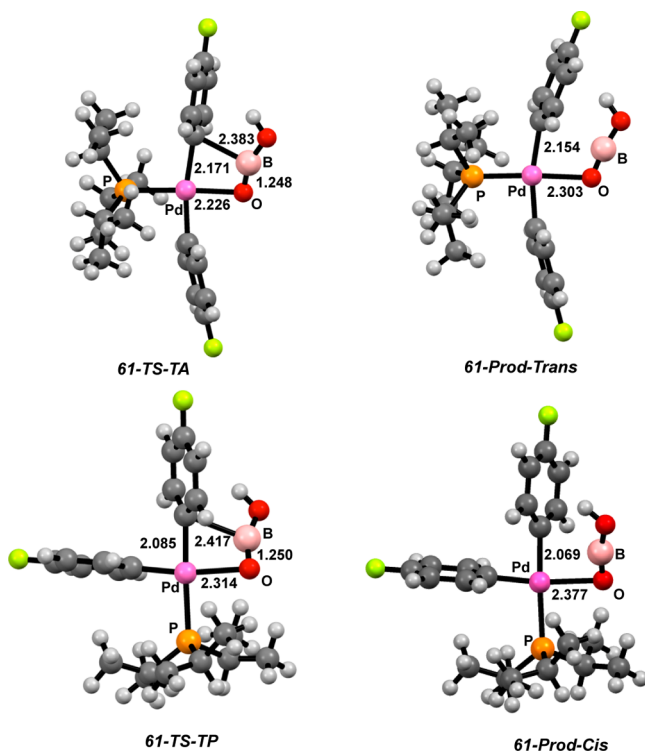


Figure 12. Transition-state and complexed product structures for transmetalation of **61**. Free energies are calculated using M062X/LANL2DZ-6-31G(d) with CPCM solvation modeling (solvent = THF) for single-point energies with thermal corrections from B3LYP/LANL2DZ-6-31G(d) at 243.15 K.

reactivity. Furthermore, a series of structural, kinetic, and computational investigations revealed two mechanistically distinct pathways: (1) transmetalation via a 6-B-3 intermediate that dominates in the presence of excess phosphine, and (2) transmetalation via an anionic 8-B-4 intermediate that

dominates in mono-ligated or *cis*-chelated systems. The observation of direct transmetalation from a tri-coordinate boron center (complex **51**) challenges the current dogma that boron must be activated by base prior to transmetalation. Overall, the key feature that enables the transfer of the organic fragment from boron to palladium is the availability of an empty coordination site on the palladium atom. The importance of a coordinatively unsaturated palladium atom was revealed by both the inverse first-order dependence on *i*-Pr₃P and inhibitory effects of water for the formation of cross-coupling product from the 6-B-3 intermediate **51**. The importance of a sub-ligated palladium atom was further demonstrated by the DFT calculations and rapid transmetalation observed in 8-B-4 complex **60** that contained a single *i*-Pr₃P ligand bound to palladium. Further effects of solvent, boron sources, and additives on the transmetalation event are currently under investigation and will be reported in due course.

ASSOCIATED CONTENT

S Supporting Information

The Supporting Information is available free of charge on the ACS Publications website at DOI: [10.1021/jacs.6b13384](https://doi.org/10.1021/jacs.6b13384).

Full experimental procedures and characterization data and copies of ¹H, ¹³C, ³¹P, ¹⁹F, ¹¹B, NOESY, and EXSY spectra, along with full kinetic data ([PDF](#))

AUTHOR INFORMATION

Corresponding Author

*sdenmark@illinois.edu

ORCID

Andy A. Thomas: [0000-0001-6336-5566](https://orcid.org/0000-0001-6336-5566)

Scott E. Denmark: [0000-0002-1099-9765](https://orcid.org/0000-0002-1099-9765)

Notes

The authors declare no competing financial interest.

ACKNOWLEDGMENTS

We are grateful for generous financial support from the National Science Foundation (CHE1012663 and CHE1151566). A.A.T. is grateful to the University of Illinois and Eli Lilly for Graduate Fellowships. Dr. Lingyang Zhu is thanked for helpful suggestions on NMR spectroscopy. Some of this data was collected in the Core Facilities at the Carl R. Woese Institute for Genomic Biology on a 600 MHz NMR funded by NIH grant number S10-RR028833 and the Integrated Molecular Structure Education and Research Center at Northwestern University.

REFERENCES

- (1) (a) Chemla, F.; Ferreira, F.; Perez-Luna, A.; Micouin, L.; Jackowski, O. In *Metal-Catalyzed Cross-Coupling Reactions and More*, 3rd ed.; de Meijere, A., Bräse, S., Oestreich, M., Eds.; Wiley-VCH: Weinheim, Germany, 2014; Vol. 1, Chapter 5. (b) Heravi, M. M.; Hajiabbasi, P. *Monatsh. Chem.* **2012**, *143*, 1575–1592.
- (2) (a) Lee, J. C. H.; Hall, D. G. In *Metal-Catalyzed Cross-Coupling Reactions and More*, 3rd ed.; de Meijere, A., Bräse, S., Oestreich, M., Eds.; Wiley-VCH: Weinheim, Germany, 2014; Vol. 1, Chapter 2. (b) Lennox, A. J. J.; Lloyd-Jones, G. C. *Chem. Soc. Rev.* **2014**, *43*, 412–443. (c) Miyaura, N.; Suzuki, A. *Chem. Rev.* **1995**, *95*, 2457–2483.
- (3) (a) Martín-Matute, B.; Szabó, K. J.; Mitchell, T. N. In *Metal-Catalyzed Cross-Coupling Reactions and More*, 3rd ed.; de Meijere, A., Bräse, S., Oestreich, M., Eds.; Wiley-VCH: Weinheim, Germany, 2014; Vol. 2, Chapter 6. (b) Farina, V.; Krishnamurthy, V.; Scott, W. J. *Org. React.* **1997**, *50*, 1.
- (4) (a) Chang, W. T. T.; Smith, R. C.; Regens, C. S.; Bailey, A. D.; Werner, N. S.; Denmark, S. E. *Org. React.* **2011**, *75*, 213. (b) Denmark, S. E.; Sweis, R. F. In *Metal-Catalyzed Cross-Coupling Reactions and More*, 3rd ed.; de Meijere, A., Bräse, S., Oestreich, M., Eds.; Wiley-VCH: Weinheim, Germany, 2014; Vol. 2, Chapter 7.
- (5) (a) Xu, S.; Kamada, H.; Kim, E. H.; Oda, A.; Negishi, E. In *Metal-Catalyzed Cross-Coupling Reactions and More*, 3rd ed.; de Meijere, A., Bräse, S., Oestreich, M., Eds.; Wiley-VCH: Weinheim, Germany, 2014; Vol. 1, Chapter 3. (b) Phapale, V. B.; Cárdenas, D. *J. Chem. Soc. Rev.* **2009**, *38*, 1598–1607.
- (6) (a) Suzuki, A. *Angew. Chem., Int. Ed.* **2011**, *50*, 6722–6737. (b) Seechurn, C. C. C. J.; Kitching, M. O.; Colacot, T. J.; Snieckus, V. *Angew. Chem., Int. Ed.* **2012**, *51*, 5062–5085.
- (7) Picquet, M. In *Organometallics as Catalysts in the Fine Chemical Industry*; Matthias, B., Blaser, H. U., Eds.; Springer: Berlin/Heidelberg, 2013; Vol. 42, Chapter 1.
- (8) (a) Magano, J.; Dunetz, J. R. *Chem. Rev.* **2011**, *111*, 2177–2250. (b) Torborg, C.; Beller, M. *Adv. Synth. Catal.* **2009**, *351*, 3027–3043. (c) Corbet, J.-P.; Mignani, G. *Chem. Rev.* **2006**, *106*, 2651–2710. (d) Lipton, M. F.; Mauragis, M. A.; Maloney, M. T.; Veley, M. F.; VanderBor, D. W.; Newby, J. J.; Appell, R. B.; Daugs, E. D. *Org. Process Res. Dev.* **2003**, *7*, 385–392.
- (9) For leading texts on this subject, see: (a) Labinger, J. A. *Organometallics* **2015**, *34*, 4784–4795. (b) Hartwig, J. F. *Organotransition Metal Chemistry: From Bonding to Catalysis*; University Science Books: Sausalito, CA, 2010. (c) Collman, J. P.; Hegedus, L. S. *Principles and Applications of Organotransition Metal Chemistry*; University Science Books: Mill Valley, CA, 1980.
- (10) (a) Hartwig, J. F. *Inorg. Chem.* **2007**, *46*, 1936–1947. (b) Procelewska, J.; Zahl, A.; Liehr, G.; van Eldik, R.; Smythe, N. A.; Williams, B. S.; Goldberg, K. L. *Inorg. Chem.* **2005**, *44*, 7732–7742. (c) Shekhar, S.; Hartwig, J. F. *J. Am. Chem. Soc.* **2004**, *126*, 13016–13027. (d) Hartwig, J. F. *Acc. Chem. Res.* **1998**, *31*, 852–860. (e) Komiya, S.; Albright, T. A.; Hoffmann, R.; Kochi, J. K. *J. Am. Chem. Soc.* **1976**, *98*, 7255–7265.
- (11) Labadie, J. W.; Stille, J. K. *J. Am. Chem. Soc.* **1983**, *105*, 6129–6137.
- (12) (a) Tymonko, S. A.; Smith, R. C.; Ambrosi, A.; Denmark, S. E. *J. Am. Chem. Soc.* **2015**, *137*, 6192–9199. (b) Tymonko, S. A.; Smith, R. C.; Ambrosi, A.; Ober, M. H.; Wang, H.; Denmark, S. E. *J. Am. Chem. Soc.* **2015**, *137*, 6200–6218.
- (13) (a) Schmidt, A. F.; Kurokhtina, A. A.; Smirnov, V. V.; Larina, E. V.; Chechil, E. V. *Kinet. Catal.* **2012**, *53*, 214–221. (b) Zim, D.; Lando, V. R.; Dupont, J.; Monteiro, A. L. *Org. Lett.* **2001**, *3*, 3049–3051. (c) Moreno-Mañas, M.; Pérez, M.; Pleixats, R. *J. Org. Chem.* **1996**, *61*, 2346–2351.
- (14) For an excellent summary of the current state of understanding of transmetalation in the Suzuki–Miyaura reaction, see: Lennox, A. J. J.; Lloyd-Jones, G. C. *Angew. Chem., Int. Ed.* **2013**, *52*, 7362–7370.
- (15) Strictly speaking, other transmetalation pathways are possible with organoboron derivatives that do not require pre-association: (a) Ohmura, T.; Awano, T.; Sugino, M. *J. Am. Chem. Soc.* **2010**, *132*, 13191–13193. (b) Sandrock, D.; Jean-Gérard, L.; Chen, C. Y.; Dreher, S. D.; Molander, G. A. *J. Am. Chem. Soc.* **2010**, *132*, 17108–17110. (c) Lee, J. C. H.; McDonald, R.; Hall, D. G. *Nat. Chem.* **2011**, *3*, 894–899.
- (16) (a) Miyaura, N.; Yamada, K.; Suzuki, A. *Tetrahedron Lett.* **1979**, *20*, 3437–3440. (b) Miyaura, N.; Suzuki, A. *J. Chem. Soc., Chem. Commun.* **1979**, 866–867.
- (17) The use of pre-formed tetracoordinate metal boronates as cross-coupling partners has gained much attention over the past decade due to the ease of their preparation and isolation. The advantage of using pre-formed metal trihydroxyborates $\text{RB}(\text{OH})_3^-$ is that no additional base is necessary: Cammidge, A. N.; Goddard, V. H. M.; Gopee, H.; Harrison, N. L.; Hughes, D. L.; Schubert, C. J.; Sutton, B. M.; Watts, G. L.; Whitehead, A. *Org. Lett.* **2006**, *8*, 4071–4074.
- (18) Miyaura, N.; Yamada, K.; Sugino, M.; Suzuki, A. *J. Am. Chem. Soc.* **1985**, *107*, 972–980.
- (19) Matos, K.; Soderquist, J. A. *J. Org. Chem.* **1998**, *63*, 461–470.
- (20) Ortuño, M. A.; Lledós, A.; Maseras, F.; Ujaque, G. *ChemCatChem* **2014**, *6*, 3132–3138.
- (21) These conclusions have also been reached in similar DFT investigations: (a) Sicre, C.; Braga, A. A. C.; Maseras, F.; Cid, M. M. *Tetrahedron* **2008**, *64*, 7437–7443. (b) Sumimoto, M.; Iwane, N.; Takahama, T.; Sakaki, S. *J. Am. Chem. Soc.* **2004**, *126*, 10457–10471. (c) Goossen, L. J.; Koley, D.; Hermann, H. J.; Thiel, W. *J. Am. Chem. Soc.* **2005**, *127*, 11102–11114. (d) Goossen, L. J.; Koley, D.; Hermann, H. L.; Thiel, W. *Organometallics* **2006**, *25*, 54–67.
- (22) Jover, J.; Fey, N.; Purdie, M.; Lloyd-Jones, G. C.; Harvey, J. N. J. *Mol. Catal. A: Chem.* **2010**, *324*, 39–47.
- (23) Carrow, B. P.; Hartwig, J. F. *J. Am. Chem. Soc.* **2011**, *133*, 2116–2119.
- (24) (a) Amatore, C.; Jutand, A.; Le Duc, G. *Chem. - Eur. J.* **2011**, *17*, 2492–2503. (b) Amatore, C.; Jutand, A.; Le Duc, G. *Angew. Chem.* **2012**, *124*, 1408–1411.
- (25) Schmidt, A. F.; Kurokhtina, A. A.; Larina, E. V. *Russ. J. Gen. Chem.* **2011**, *81*, 1573–1574.
- (26) $(\text{Ph}_3\text{P})_2\text{PdPhOH}$ was generated *in situ* by reacting $[(\text{Ph}_3\text{P})\text{PdPh}(\text{OH})]_2$ in the presence of excess Ph_3P .
- (27) Aliprantis, A. O.; Canary, J. W. *J. Am. Chem. Soc.* **1994**, *116*, 6985–6986.
- (28) Pantcheva, I.; Nishihara, Y.; Osakada, K. *Organometallics* **2005**, *24*, 3815–3817.
- (29) Zhao, P.; Incarvito, C. D.; Hartwig, J. F. *J. Am. Chem. Soc.* **2007**, *129*, 1876–1877.
- (30) (a) Denmark, S. E.; Williams, B. J.; Eklov, B. M.; Pham, S. M.; Beutner, G. L. *J. Org. Chem.* **2010**, *75*, 5558–5572. (b) Bartholomew, E. R.; Bertz, S. H.; Cope, S. K.; Murphy, M. D.; Ogle, C. A.; Thomas, A. A. *Chem. Commun.* **2010**, *46*, 1253–1254.
- (31) McGarry, J. F.; Prodolliet, J.; Smyth, T. *Org. Magn. Reson.* **1981**, *17*, 59–65.
- (32) A preliminary communication describing some of these results has already appeared: Thomas, A. A.; Denmark, S. E. *Science* **2016**, *352*, 329–332.
- (33) Butters, M.; Harvey, J. N.; Jover, J.; Lennox, A. J. J.; Lloyd-Jones, G. C.; Murray, P. M. *Angew. Chem., Int. Ed.* **2010**, *49*, 5156–5160.
- (34) For a complete, tabular listing of all chemical shifts, see the Supporting Information.

- (35) Grushin, V. V.; Alper, H. *Organometallics* **1996**, *15*, 5242–5245.
- (36) In the absence of excess *i*-Pr₃P, the cross-coupling product **53** was observed.
- (37) Nishihara, Y.; Onodera, H.; Osakada, K. *Chem. Commun.* **2004**, 192–193.
- (38) This classification designates *N*-X-L species where *N* is the number of formally valence-shell electrons about atom X, involved in bonding L ligands to X: Perkins, C. W.; Martin, J. C.; Arduengo, A. J.; Lau, W.; Alegria, A.; Kochi, J. K. *J. Am. Chem. Soc.* **1980**, *102*, 7753–7759.
- (39) Weber, E.; Skobridis, K.; Ouchi, M.; Hakushi, T.; Inoue, Y. *Bull. Chem. Soc. Jpn.* **1990**, *63*, 3670–3677.
- (40) Driver, M. S.; Hartwig, J. F. *Organometallics* **1997**, *16*, 5706–5715.
- (41) Complex **62** exists as a mixture of *cis* and *trans* dimers as observed by Grushin (see ref 35).
- (42) For related 2:1 palladium complexes with acetate ligands, see: Stephenson, T. A.; Morehouse, S. M., Mrs.; Powell, A. R.; Heffer, J. P.; Wilkinson, G. *J. Chem. Soc.* **1965**, 3632–3640.
- (43) To confirm the conclusion of a direct displacement of halide from **64** with **56**, a control experiment was performed by combining **62** with **56** at –50 °C for 1 h, whereupon only trace conversion (<5%) was observed by ¹⁹F and ³¹P NMR spectroscopy.
- (44) See Supporting Information for details.
- (45) Methanol was chosen over water due to the low temperatures needed for intermediate formation. Characterization experiments were performed using THF-*d*₈ mixed with either CH₃OH or CD₃OD.
- (46) Addition of methanol (60 μL) to a THF solution of complex **63** at –78 °C followed by warming to –60 °C resulted in a quantitative conversion to both **68** and **62** in a ratio of 1:0.5, indicating that Pd-(μ-OH)-Pd is not broken by methanol.
- (47) A solution of arylboronic acid **47** in THF/CH₃OH (10:1) displays a ¹¹B NMR signal at 30 ppm, indicating that methanol is not sufficiently Lewis basic to coordinate to the boron atom.
- (48) Brown, H. C. *J. Am. Chem. Soc.* **1945**, *67*, 374–378.
- (49) Hayashi, Y.; Wada, S.; Yamashita, M.; Nozaki, K. *Organometallics* **2012**, *31*, 1073–1081.
- (50) Schott, D.; Pregosin, P. S.; Veiros, L.; Calhorda, M. J. *Organometallics* **2005**, *24*, 5710–5717.
- (51) The lack of a measurable ¹¹B NMR chemical shift prohibits the unambiguous determination of a tri- or tetracoordinate boron atom.
- (52) As described in section 3.1.7, it is not possible to confirm this assertion spectroscopically because of the rapid exchange among **47**, **60**, and **63** at –30 °C and the resulting coincidence of their NMR signals.
- (53) Although complex **60** could not be characterized spectroscopically, in section 3.2.1, it was demonstrated to be the active transmetalating species in pure THF. Therefore, the identity of Ph₃P complex **73** is inferred on the basis of the observation of similar reactivity in THF.
- (54) This conclusion is supported by the observation of a positive rho value for a Hammett study on the transmetalation step in the related cross-coupling of arylsilanlates. See: Denmark, S. E.; Smith, R. C.; Chang, W.-T. T. *Tetrahedron* **2011**, *67*, 4391–4396.
- (55) Schmid, R.; Sapunov, V. N. In *Non-Formal Kinetics in Search for Chemical Reaction Pathways*; Ebel, H. F., Ed.; Verlag Chemie: Weinheim, 1982; Vol. 14, Chapter 3.
- (56) Kuran, W.; Musco, A. *Inorg. Chim. Acta* **1975**, *12*, 187–193.
- (57) The complexity of the autocatalytic system lends itself to other possible interpretations. We offer an explanation that is most consistent with all of the available data, but we cannot unambiguously exclude the possibility that, in the presence of water, the transmetalation may still be proceeding through 8-B-4 species **60**.
- (58) In addition to **61**, approximately 25% of cross-coupling product **53** was observed.
- (59) Appleton, T. G.; Clark, H. C.; Manzer, L. E. *Coord. Chem. Rev.* **1973**, *10*, 335–422.
- (60) This energy difference is also reflected in the greater Pd-C(ipso)B bond distances in both **60**-InterTS-TA and **60**-Inter-TA (2.945 and 2.844 Å) compared to **60**-InterTS-TP and **60**-Inter-TP (2.647 and 2.418 Å).
- (61) The enthalpic contributions to the transition-state energies is much closer, as shown in Table 1, and is a more reliable measure of the bonding contributions.
- (62) Tatsumi, K.; Hoffmann, R.; Yamamoto, A.; Stille, J. K. *Bull. Chem. Soc. Jpn.* **1981**, *54*, 1857–1867.
- (63) The switch in relative energies for the Pd–O bond-breaking transition states for **61** vs **60** is again clearly reflected in the Pd–C(ipso)B bond distances. The significantly greater distances in both **61**-InterTS-TA and **61**-InterTS-TP (3.929 and 3.689 Å) compared to **60**-InterTS-TA and **60**-InterTS-TP (2.945 and 2.647 Å) support the conclusion that the steric contribution of the phosphine ligand is attenuated in the **61**-InterTS structures.
- (64) The same strategy was used in the computational analysis of cross-coupling of arylpalladium arylsilanlates to account for the high-energy dimethylsilanone species formed directly from transmetalation.^{12b}